DYNAMICS OF THE LORENZ EQUATION AND THE CHUA'S EQUATION: A TUTORIAL

by

Lj. Kocarev and T. Roska

Memorandum No. UCB/ERL M93/24

15 March 1993

ELECTRONICS RESEARCH LABORATORY

College of Engineering
University of California, Berkeley
94720

This work is supported in part by the Office of Naval Research under grant N00014-89-J-1402 and the National Science Foundation under grant MIP-9001336.

DYNAMICS OF THE LORENZ EQUATION AND THE CHUA'S EQUATION: A TUTORIAL

by

Lj. Kocarev and T. Roska

Memorandum No. UCB/ERL M93/24

15 March 1993

ELECTRONICS RESEARCH LABORATORY

College of Engineering
University of California, Berkeley
94720

This work is supported in part by the Office of Naval Research under grant N00014-89-J-1402 and the National Science Foundation under grant MIP-9001336.

DYNAMICS OF THE LORENZ EQUATION AND THE CHUA'S EQUATION: A TUTORIAL

by

Lj. Kocarev and T. Roska

Memorandum No. UCB/ERL M93/24

15 March 1993

DYNAMICS OF THE LORENZ EQUATION AND THE CHUA'S EQUATION: A TUTORIAL

by

Lj. Kocarev and T. Roska

Memorandum No. UCB/ERL M93/24

15 March 1993

ELECTRONICS RESEARCH LABORATORY

College of Engineering
University of California, Berkeley
94720

This work is supported in part by the Office of Naval Research under grant N00014-89-J-1402 and the National Science Foundation under grant MIP-9001336.

Dynamics of the Lorenz Equation and the Chua's equation: A Tutorial

Lj. Kocarev

Faculty of Electrical Engineering, Cyril and Methodius University,
Skopje, Po Box 574, Republic of Macedonia

T. Roska

Computer and Automation Institute of
the Hungarian Academy of Sciences, Budapest H 1014, Hungary

Abstract

In this paper a comparative study of the Lorenz equation and Chua's equation is presented.

1 Introduction

Within the last 20 years, the study of experimental, computational, and theoretical aspects of chaos in nonlinear dynamical systems has influenced tremendously the foundations of applied sciences and engineering so that it has become possible to understand better many complex nonlinear phenomena. Two dynamical systems have played a crucial role in this scientific development: Lorenz model [1] and Chua's circuit [2]. In this paper we shall present a comparative study of these two systems.

1.1 Lorenz Model

Lorenz's purpose was to analyze the unpredictable behavior of the weather. He first expanded a set of nonlinear partial differential equations (Navier - Stokes equation and the thermal equation) by Fourier transformations and then truncated them by retaining only three modes. The resulting equations, generally called the Lorenz equation, consists of an autonomous nonlinear system of 3 ordinary differential equations:

$$\left.\begin{aligned} \dot{x} &= \sigma(y-x) \\ \dot{y} &= rx - y - xz \\ \dot{z} &= xy - bz \end{aligned}\right\} \tag{1}$$

There are two nonlinearities in the Lorenz equations; both are functions of *two* variables, namely, xz and xy, and there are three control parameters; namely, σ, r and b. Roughly speaking, the variable x measures the rate of convective overturning, the variable y measures the horizontal temperature variation, and the variable z measures the vertical temperature

variation. The parameters σ and r are proportional to the Prandtl and the Rayleigh number, respectively. A typical Lorenz attractor is shown on Figure 1, where $\sigma = 10$, $b = 8/3$, and $r = 28$.

The relationship between the complicated turbulent behavior in systems having an infinite number of degrees of freedom (partial differential equations) and the chaotic behavior in *finite-dimensional* systems is a deep and yet unresolved problem. Lorenz himself admits that (1) is not a realistic model if r is far from 1 (as in the case of the Lorenz attractor). However, many authors have derived (1) from other physical systems. Haken [3] has used the Lorenz equation to model the irregular spiking phenomena in lasers. Malkus [4] and Yorke and Yorke [5] have used (1) to study the problem of convection in a toroidal region, while Knobloch [6] has derived (1) from a disc dynamo. Pedlosky and Frenzen [7] have derived (1) from a study of the dynamics of a weakly unstable, finite amplitude, baroclinic wave (two-layer model). Lorenz equation has also been used to describe the dynamics of the simplest laser model (e.g., the Shimizu - Morioka System [8]).

1.2 Chua's circuit

Chua's purpose was to synthesize the simplest autonomous electronic circuit generator of chaotic signals. The history on the conception of the circuit, shown in Figure 2(a), is symmarized in Ref.9. The state equations are:

$$\left.\begin{aligned} C_1\frac{dv_1}{dt} &= G(v_2 - v_1) - g(v_1) \\ C_2\frac{dv_2}{dt} &= G(v_1 - v_2) + i_3 \\ L\frac{di_3}{dt} &= -v_2 \end{aligned}\right\} \tag{2}$$

where v_1,v_2 and i_3 denote the voltage across the capacitor C_1, the voltage across the capacitor C_2 and the current through the inductor L, respectively, and $g(v_1)$, shown in Figure 2(b), is the voltage versus current characteristic of the nonlinear element, generally referred to as Chua's diode in the literature.

In contrast to the Lorenz equation which has *two* nonlinearities, each one being a scalar function of *two* variables, Chua's circuit has only *one* nonlinearity; namely, a scalar function of only *one* variable. The relevant nonlinear function in the original Chua's circuit is described by an odd-symmetric piecewise-linear function made of three straight-line segments, and which has the following *explicit* represention:

$$g(v_1) = G_b v_1 + \frac{1}{2}(G_a - G_b)(|v_1 + B_p| - |v_1 - B_p|) \tag{3}$$

It is easy to realize (2) by a physical circuit. All of the *linear* elements (capacitor, resistor, and inductor) are readily available. Several practical implementions of the *nonlinear* element (Chua's diode) can be chosen. All of them made use of only off-the-shelf components, e.g., diodes [1], transistors [10], operational amplifiers [11], and operational transconductance amplifiers [12]. One attractive feature of Chua's circuit is that it is easy to build, easy to measure, and easy to model. Because of its simplicity, robustness and low cost, Chua's circuit has become a favorite tool for analytical, numerical and experimental study of chaotic phenonena.

1.3 Physical systems versus analog computers

We would like to stress at the outset that Chua's circuit is *not* an analog computer, as is often mistakenly identified by those who had been exposed to analog computers made from operational amplifiers. In other words, while electronic analog computers are made from op amps, only a small subset of op-amp circuits are analog computers. The building blocks of Chua's circuit are ordinary circuit elements; namely, resistors, inductors and capacitors. They are not op amp integrators, the building blocks of electronic analog computers. The only nonlinear element in Chua's circuit can be realized by a variety of methods, including a thumb-nail sized integrated circuit chip with only 2 external terminals which gives the nonlinear voltage-current characteristics, and two other terminals for the battery [12]. In the dynamics of the circuit, both the current and the voltage of each circuit element play a crucial role. On the other hand, the variables in an analog computer are merely the node voltages of the capacitor – integrator building block modules where the *current* is completely irrelevant in the circuit's dynamic operation and is in fact forced to a near-zero value in order to avoid loading effects which would otherwise affect the analog relationships being simulated. In the language of system theory, an analog computer is only an electronic implementation of a *signal flow graph* where the notion of power flow and energy has no meaning. In contrast, Chua's circuit is a *physical* system obeying *electrical* (Kirchhoff's) laws, just like a mechanical spring-mass-dashpot systm obeying *mechanical* (Newton's) laws. If we simulate the equations of motion of the mechanical system by a system of op-amp integrators, then the resulting electronic system is an *analog computer.* But the mechanical system itself is a physical system.

2 Lorenz and Chua's equations

Introducing the dimensionless variables,

$$\begin{array}{lll} \mathrm{x} \triangleq \frac{v_1}{B_p} & \mathrm{y} \triangleq \frac{v_2}{B_p} & \mathrm{z} \triangleq \frac{i_3}{B_p} \\ \tau \triangleq \frac{tG}{C_2} & \mathrm{a} \triangleq \frac{G_a}{G} & \mathrm{b} \triangleq \frac{G_b}{G} \\ \alpha \triangleq \frac{C_2}{C_1} & \beta \triangleq \frac{C_2}{LG^2} & \end{array}$$

Equation (3) can be transformed into the following dimensionless form:

$$\left.\begin{array}{rcl} \frac{dx}{d\tau} & = & \alpha(y - x - f(x)) \\ \frac{dy}{d\tau} & = & x - y + z \\ \frac{dz}{d\tau} & = & -\beta y \end{array}\right\} \qquad (4)$$

where

$$\begin{aligned} f(x) &\triangleq g(x; 1, b, a) \\ &= \begin{cases} bx + a - b & x \geq 1 \\ ax & |x| \leq 1 \\ bx - a + b & x \leq -1 \end{cases} \end{aligned}$$

and α, β, a and b are real parameters, $\alpha > 0$, $\beta > 0$, $a < 0$ and $b < 0$.

Figure 3 shows a typical double-scroll Chua's attractor observed by solving (4) with α = 9, $\beta = 14\frac{2}{7}$, a = $-\frac{8}{7}$, b = $-\frac{5}{7}$.

We will now compare the dynamics of the Lorenz equation (1) and Chua's equation (4).

2.1 Simple properties

2.1.1 Lorenz equation

Equation (1) is invariant under the transformation

$$(x, y, z) \rightarrow (-x, -y, -z)$$

The origin is an equilibrium point for all parameter values. For $r>1$ there are two other equilibrium points :

$$\begin{aligned} P^+ &= (\sqrt{b(r-1)}, \sqrt{b(r-1)}, r-1) \\ P^- &= (-\sqrt{b(r-1)}, -\sqrt{b(r-1)}, r-1) \end{aligned}$$

The linearized flow near the origin has eigenvalues:

$$\begin{aligned} \lambda_1, \lambda_2 &= \frac{1}{2}\{-\sigma - 1 \pm \sqrt{(\sigma-1)^2 + 4\sigma r}\} \\ \lambda_3 &= -b \end{aligned}$$

The eigenvalues of the flow linearized near P^+ and P^- are the roots of the equation

$$s^3 + s^2(\sigma + b + 1) + sb(\sigma + r) + 2\sigma b(r-1) = 0$$

The equilibrium points are stable iff:

$$\sigma + b + 1 > 0, \quad b(\sigma + r) > 0, \quad \sigma b(r-1) > 0, \quad \text{and} \quad (\sigma + b + 1)b(\sigma + r) > \sigma b(r-1)$$

For the values of parameters in the neighborhood of $\sigma = 10$, $b = 8/3$, $r = 28$, all equilibrium points are hyperbolic, i.e., the flow linearized around the origin has two negative, and one positive, *real* eigenvalues; the flow linearized around P^+ (P^-) has one negative real eigenvalue and a complex-conjugate pair of eigenvalues with a positive real part, as shown in Fig. 4(a). A typical trajectory in a small neighborhood of each equilibrium point is shown in Fig. 4(b).

2.1.2 Chua's equation

Equation (4) is invariant under the transformation

$$(x, y, z) \rightarrow (-x, -y, -z)$$

The origin is an equilibrium point. For a $\neq$ b, b $\neq$ -1, and $(a+1)(b+1) < 0$, there are two other equilibrium points:

$$\begin{aligned} P^+ &= \left(\frac{b-a}{b+1}, 0, -\frac{b-a}{b+1} \right) \\ P^- &= \left(-\frac{b-a}{b+1}, 0, \frac{b-a}{b+1} \right) \end{aligned}$$

The eigenvalues of the flow linearized near each equilibrium point are the roots of the equation:

$$s^3 + s^2(\alpha c + \alpha + 1) + s(\alpha c + \beta) + \beta\alpha(c+1) \;=\; 0$$

where c is equal to a if the equilibrium point is at the origin, and c is equal to b if the equilibrium point is at P^+ (or P^-). The equilibrium points are stable iff:

$$\alpha c + \alpha + 1 > 0, \;\; \alpha c + \beta > 0, \;\; \alpha(c+1) > 0, \;\; \text{and} \;\; (\alpha c + \alpha + 1)(\alpha c + \beta) > \alpha(c+1)$$

For the values of parameters in a neighborhood of $\alpha = 9$, $\beta = 14\frac{2}{7}$, a = $-\frac{8}{7}$, b = $-\frac{5}{7}$, all equilibrium points are hyperbolic; the flow linearized around the origin has one positive real eigenvalue, and a complex conjugate pair of eigenvalues with negative real part. The flow linearized around P^+ (P^-) has one negative real eigenvalue, and a complex-conjugate pair of eigenvalues with positive real part, as shown in Fig. 5(a). A typical trajectory in a small neighborhood of each equilibrium point is shown in Fig. 5(b).

In what follows we shall asume that

$$\sigma = 10, b = 8/3 \qquad \text{for Lorenz equation}$$

and

$$a = -8/7, b = -5/7 \qquad \text{for Chua's equation.}$$

2.2 Homoclinic and heteroclinic orbits

A *homoclinic orbit* of an equilibrium point is a trajectory which tends to the equilibrium point in both forward and reverse time. Figure 6 shows a schematic "number 8" homoclinic orbit of the origin for Lorenz equation when $r = 13.926$. Figure 7 shows a schematic "double scroll" homoclinic orbit of the origin for Chua's equation when $\alpha = 11.0917459$, $\beta = 14\frac{2}{7}$.

A *heteroclinic orbit* between the two equilibrium points P^* and Q^* is a trajectory which tends towards P^* in reverse time and towards Q^* in forward time. Many heteroclinic orbits for the Lorenz and the Chua's equation can be found in Ref.13 and Ref.14, respectively.

2.3 Period doubling

Over various ranges of parameter values both equations (1) and (4) display a *period - doubling bifurcation* phenomenon. Here we present an example of *such a bifurcation* sequence, in Figure 8 for Lorenz equation and in Figure 9 for Chua's equation.

2.4 Intermittent chaos

By *intermittency* we mean the occurrence of a signal which alternates randomly between long regular (laminar) phases and relatively short irregular bursts.

This phenomenon is observed in the Lorenz equation for $r = 166.3$, as shown in Figure 10, and in Chua's equation for $\alpha = 4.295$, $\beta = 5$, as shown in Figure 11.

2.5 Meta-stable chaos

A phenomenon is called "*preturbulence*" or "*meta-stable chaos*" when a typical dynamical system trajectory wanders chaotically near a *strange* set before it is attracted into a non-chaotic attractor (usually a fixed point or a periodic orbit).

Figure 12 shows this phenomenon in Lorenz equatin for r= 22.4, while Figure 13 shows this phenomenon in Chua's equation for the parameters: α = 8.986, $\beta = 14\frac{2}{7}$. The steady state is a *fixed point* for Lorenz equation, and a *periodic orbit* for Chua's circuit.

2.6 Semi-periodicity

Suppose that for some suitable Poincare plane of a three-dimensional flow we can locate "n" non-overlapping connected component regions on the plane such that all trajectories eventually pass through these regions in a cyclic order. Then we say that the system is *semi-periodic* with period n.

Figure 14(a) shows the semi-periodicity in Lorenz equation for r = 212, while Figure 15(a) shows this phenomenon in Chua's equation for the parameters: α = 8.99, $\beta = 14\frac{2}{7}$. The Poincare cross section at x = 20 shown in Fig. 14(b) depicts only one isolated component (n = 1). The corresponding cross section at x = 1 shown in Fig. 15(b) depicts two isolated components (n = 2). Both figures show that the behaviour of the corresponding equation looks almost like stable periodic behaviour, though it can be shown that the periodic orbit in question lost its stability in a period-doubling bifurcation. In fact, the attractor is constrained within a tube that surrounds a hyperbolic periodic orbit of period n. The tubes are very thin and they intersect some appropriately chosen return plane in n non-overlapping regions.

2.7 Co-existing attractors

Figure 16 shows two co-existing chaotic attractors in the Lorenz equations for r = 212, and Figure 17 shows three co-existing chaotic attractors in the Chua's equations for α = 15.6 and β = 28.58.

2.8 The Lorenz attractor and the Double-Scroll Chua's attractor

2.8.1 Lorenz equation

The Afraimovich-Bykov-Shil'nikov geometric model [15]

Let us consider the domain U, in the space of vector fields with C^1-topology on $\mathcal{R}^3$ (we restrict ourselves for simplicity to $\mathcal{R}^3$; more general case is considered in Reference 13), such that every vector field $X \in U$ has an equilibrium state 0 of the saddle type. Here, the eigenvalues of X at the point 0 are real and satisfy $\lambda_1 < \lambda_2 < 0 < \lambda_3$ with $\lambda_2 + \lambda_3 > 0$. Denote by $W^s(x)$ the stable two-dimensional manifold of 0 and by $W^u(x)$ the unstable manifold consisting of 0 and of two trajectories Γ_1 and Γ_2, emanating from 0, in forward and in backward time, respectively. We assume that the system $X_0 \in U$ satisfies $\Gamma_i \in W^s(x_0)$ i = 1,2, that is Γ_i is doubly asymptotic to 0.

Let us assume that for every system $X \in U$ there exists an element of area D with the following properties :

1. Euclidean coordinates (x,y) can be introduced on D, where

$$D = \{(x,y)| \quad |x| \leq 1, \quad |y| \leq 2\}$$

2. The equation $y = 0$ describes the line of discontinuity, that is the intersection $W^s \cap D$

3. Mappings $T_1: D_1 \rightarrow D$ and $T_2: D_2 \rightarrow D$ are defined along the trajectories of the system, where

$$D_1 = \{(x,y)| \ |x| \leq 1, \ 0 < y \leq 1 \}$$
$$D_2 = \{(x,y)| \ |x| \leq 1, -1 \leq y < 0 \}$$

and T_i can be expressed as

$$\bar{x} = f_i(x,y)$$
$$\bar{y} = g_i(x,y)$$

$i = 1,2$. In addition the functions f and g must satisfy some conditions (Equation (1.1) in Ref.13).

The Afraimovich-Bykov-Shil'nikov model is defined by the two-dimensional map T (see Fig.18):

$$T \triangleq T_i \mid D_i \ \text{ on } D_i, \ \text{i} = 1,2.$$

This mapping gives rise to a Lorenz-like attractor; in particular it has been proved that the map T has a strange attractor.

The Birman-Williams model [16]

By a *template* in a three-dimensional manifold M is meant a branched two-manifold $B \subset M$ together with a semi-flow γ_t: $B \rightarrow B$, $t \geq 0$ such that B has an atlas consisting of 2 types of charts, a joint chart and a spliting chart.

The Birman-Williams model represents the inverse limit of a semi-flow on a branched two-dimensioned manifold. The Lorenz template is shown in Figure 19.

2.8.2 Chua's equation

The Belyhkh-Chua Geometric model [17]

Consider the class of three-dimensional, piecewise-linear system satisfying the following conditions:

1. Inside the cylinder

$$G = \{|x| \leq h \quad y^2 + z^2 \leq r^2\}$$

the system is defined by the following linear system:

$$\begin{aligned} \dot{x} &= \gamma x \\ \dot{y} &= -\sigma y - \omega_0 z \\ \dot{z} &= \omega_0 y - \sigma z \end{aligned}$$

In other words, the origin is a hyperbolic equilibrium point with one real eigenvalue $\gamma > 0$, and a pair of complex-conjugate eigenvalues $-\sigma \pm i\,\omega_0$, $\sigma > 0$.

Let us define

$$\begin{aligned} D_1 &= \{y^2 + z^2 = r^2 : 0 < x \leq h\} \\ D_2 &= \{y^2 + z^2 = r^2 : -h \leq x < 0\} \\ d_h{}^1 &= \{y^2 + z^2 \leq r^2 : x = h\} \\ d_h{}^2 &= \{y^2 + z^2 = r^2 : x = -h\} \\ D &= D_1 \cup D_2 \cup \{y^2 + z^2 = r^2 : x = 0\} \end{aligned}$$

2. Outside the cylinder G, the system generates an odd-symmetric linear Poincare map such that

$$\begin{aligned} S|_{d_h{}^1} &= S_1 : d_h{}^1 \rightarrow D \\ S|_{d_h{}^2} &= S_1 : d_h{}^2 \rightarrow D \end{aligned}$$

The Belykh-Chua model is represented by the following map f:

$$\left.\begin{aligned} \bar{\phi} &= -\tfrac{\pi}{2} + (\tfrac{\pi}{2} + a|x|^\gamma \cos(\phi + \varphi - \omega \ln|x|))\, sgn\, x \quad x \neq 0, x \in D \\ \bar{x} &= \mu\, sgn\, x - a|x|^\gamma \sin(\phi + \varphi - \omega \ln|x|)\, sgn\, x \quad x \neq 0, x \in D \end{aligned}\right\} \quad (5)$$

where γ and ω are "local" parameters, while μ, a, and φ are "global" parameters. The parameter μ controls the return points P_1 and P_2; the case $\mu = 0$ is drawn on Figure 20, in this case the separatrices Γ_1 and Γ_2 are doubly asymptotic to the origin. If $\mu > 0$, then P_1 (P_2) is translated upward (downward) by an amount equal to μ. The parameter a is usually called the separatrix value and φ is called the phase shift.

This type of mapping gives rise to a double-scroll Chua's attractor. In particular, it has been proved that the map (5) has a strange attractor.

Induced template [18]

Let φ_t:$M \rightarrow M$ be a flow on M. The flow φ_t is compatible with the induced template, if all periodic orbits embedded in the chaotic attractor are associated with the periodic orbits of the template in such a way that the braid structure is preserved. The induced template of the double-scroll Chua's attractor is shown in Figure 21.

3 Additional Features of Chua's Circuit

In this section we shall briefly discuss some additional features of Chua's circuit

3.1 Theoretical features

Equation (4) is a piecewise-linear dynamical system, and as a consequence, analytical expression for two-dimensional Poincare map has been derived [19]. It has been used for in-depth analysis of various nonlinear properties of (4), including chaotic dynamics, birth and death of the double-scroll Chua's attractor, etc. A one-dimensional approximation of the Poincare map is introduced in Reference 19. This 1-D map predicted all of the qualitative behavior that we have so far observed by computer simulation and by rigorous analysis. Recently, Kuznetsov et.al. [20] have shown the existence of a variety of types of critical points which are characterized by a universal self-similar topography using the one-dimensional map.

Figures 22 and 23 show qualitatively distinct chaotic attractors so far observed from the Lorenz and the Chua's equation, respectively. By adding a linear resistor in series with the inductor in Chua's circuit, we obtain an unfolded Chua's circuit, called the Chua's oscillator [21]. The state equation of this circuit is topologically conjugate to a 21-parameter family of continuous odd-symmetric piece-wise linear equations in $\mathcal{R}^3$. Thus, the qualitative dynamics of every autonomous 3rd-order symmetric 3-segment piecewise-linear function can be mapped into this circuit. More than 50 distinct non-periodic attractors have been found so far from this circuit. Moreover, virtually every known 3*rd* order *chaotic* autonomous system, not necessarily piecewise-linear, can be modeled by a Chua's oscillator having the same qualitative behavior.

3.2 Numerical features

Since (4) is a piecewise-linear system, in each linear region of the non-linear resistor, the differential equation representing Chua's circuit is linear. It is possible to develop a computer program to find the trajectory of (4) using explicit equations [22]. Recently, using the concept of confinors, Lozi and Ushiki [23] have devised a very accurate numerical method for the computation of the half-Poincare map, and as a consequence, for the analysis of the precise structure of chaotic attractors and bifurcation dynamics in Chua's equation.

3.3 Experimental features

The main advantage of Chua's circuit (and the unfolded Chua's circuit) over other dynamical systems, from our point of view, is that it can be used as an experimental tool as well as building block for many real-world applications. Chaotic synchronization has already been exploited in the design of secure communition systems [24], and in transmission of digital signals [25]. Several methods have been developed for controlling chaos in Chua's circuit [26–31]. Moreover, experimental evidence showing the existence of signal amplification via perturbation of periodic and chaotic orbits have been presented in Chua's circuit [32]. This result has exciting potentials for low-noise amplification and high-sensitivity detector applications.

Moreover, an integrated circuit version of Chua's diode [12] as well as Chua's circuit [33] has already been built. While there are many dynamical systems known to produce chaos, few has a simple and robust circuit realization. The Lorenz equations, for example, has a dynamical

range much larger than what is easily executable in a circuit [43]. Individual variables in these equations vary over at least three orders of magnitude. Since the largest value possible in a typical power supply voltage is 15 volts, this would cause the smallest values of the variable signals to be in the order of hundredths or thousandths of a volt, which is below the noise levels typical in circuits. Circuits for the Lorenz equations have been built often as an analog computer with several multipliers. However, they are often problematic due to the limited dynamic range of practical multipliers.

4 Concluding remarks

Lorenz model and Chua's circuit have been generalized in many directions. We shall mention here some of them. In the case of Lorenz system one direction is to define a generalized Lorenz system by considering different truncations of the convection equation. Many systems obtained in such a way have been studied: including a fourteen-dimensional system [34], a five-dimensional system [35,36], and a seven-dimensional system [37]. Another direction investigates a complex generalization of the Lorenz equation (the variables x and y are allowed to be complex, as are some parameters [38]). This equation can describe the dynamic behaviors in baroclinic instability and nonlinear optics adequately.

In the case of Chua's circuit one direction investigates higher - and infinite - dimensional systems. For example, Reference 39 uses a CNN array of Chua's circuits, Reference 40 uses a finite number of discrete lossy transmission line sections as the resonator, while References 41 and 42 use a terminated coaxial cable and a delay line as the resonator, respectively. Another direction focuses on the investigation of the unfolded Chua's circuit [21]. The significance of this circuit is that the qualitative dynamics of every autonomous 3rd-order circuit (and dynamical system) containing one odd-symmetric 3-segment piecewise-linear function can be mapped into this circuit. On the other hand, experimental observations of various nonlinear phenomena can be made by building the unfolded Chua's circuit with corresponding parameters. The negative parameters can be realized with the help of a negative impedance converter having a large enough linear dynamic range.

Both systems, Lorenz and Chua's equations have generated worldwide interests among scientists. One advantage of Chua's circuit and Chua's oscillator (unfolded Chua's circuit) over other systems is that it is the only known physical system whose mathematical model is capable of duplicating almost all experimentally observed phenomena, and which has been proved to be chaotic in a rigorous mathemaiical sense [19]. In contrast, no one has succeeded yet in proving the Lorenz equation is chaotic: only its approximated 2-D map, *not* the original ODE, has so far been proved to be chaotic.

References

[1] E. N. Lorenz. Deterministic non-periodic flows. *J. Atmos. Sc.,*, 20:130–141, 1963.

[2] T.Matsumoto. A chaotic attractor from Chua's circuit. *IEEE Trans CAS*, 31(12):1055–1058, 1984.

[3] H. Haken. Analogy between higher instabilities in fluids and lasers. *Phys. Lett.*, 53(A):77–78, 1975.

[4] W. V. R. Malkus. Non-periodic convention at high and low Prandtl number. *Memoires Societe Royale des Sciences de Lige, Series, 6,*, IV:125–128, 1972.

[5] E. D. Yorke and J. A. Yorke. Metastable chaos: transition to sustained chaotic behaviour in the Lorenz model. *J. Stat. Phys.,*, 21(3):263–277, 1979.

[6] E. Knobloch. Chaos in a segmented disc dynamo. *Phys. Lett.,*, 82(A):439–440, 1981.

[7] J. Pedlosky and C. Frenzen. Chaotic and periodic behaviour of finite amplitude baroclinic waves. *J. Atmos. Sc.,*, 37:1171–1196, 1980.

[8] T. Shimizu and N. Morioka. Chaos and limit cycles in the Lorenz equations. *Phys. Lett.,*, 66(A):182–184, 1978.

[9] L.O.Chua. The genesis of Chua's circuit. *Archiv fur Elektronik und Ubertragungstechnik*, 46(4):250–257, 1992.

[10] G.Q. Zhong and F. Ayrom. Experimental confirmation of chaos from Chua's circuit. *Int.J. of Circuit Theory and Applications*, 13(1):93–98, 1985.

[11] T.Matsumoto, L. O. Chua, and K. Tokumasu. Double scroll via a two-transistor circuit. *IEEE Trans CAS*, 33(8):828–835, 1986.

[12] J. Cruz and L. O. Chua. A CMOS IC nonlinear resistor for Chua's circuit. *IEEE Trans. on CAS*, 39(12):985–995, 1992.

[13] C. Sparrow. *THe Lorenz equation: Bifurcations, Chaos, and Strange Attractors.* Springer-Verlag, New York, 18982.

[14] M. Komuro, R. Tokunaga, T. Matsumoto, and A. Hotta. Global bifurcation analysis of the double scroll circuit. *Int. J. of Bifurcation and Chaos*, 1(1):139–182, 1991.

[15] V. S. Afraimovich, V. V. Bykov, and L. P. Shil'nikov. On structurally unstable attracting limit sets of Lorenz attractor type. *Transactions of the Moscow Society*, 44:153–216, 1983.

[16] J. S. Birman and R. F. Williams. Knotted periodic orbits in dynamical systems I: Lorenz equations. *Topology*, 22:47–82, 1983.

[17] V.N. Belykh and L.O. Chua. New type of strange attractor from a geometric model of Chua's circuit. *Int. J. of Bifurcation and Chaos*, 2(3):697–704, Sept 1992.

[18] Lj. Kocarev, D. Dimovski., Z. Tasev, and L. O. Chua. Induced template for the double-scroll Chua's attractor. in preparation.

[19] L.O.Chua, M.Komuro, and T.Matsumoto. The double scroll family, parts I and II. *IEEE Trans CAS*, 33(11):1073–1118, 1986.

[20] A. P. Kuznetsov, S. P. Kuznetsov, I. R. Sataev, and L. O. Chua. Self-similarity and universality in Chua's circuit. *J. of Circuits, Systems and Computers*, 3(2), June 1993.

[21] L.O. Chua. Global unfolding of Chua's Circuits. *IEICE Trans. on Fundamentals of Electronics, Communication and computer sciences, Special Issue on Neural nets, chaos and numerics*, May, 1993.

[22] L.O. Chua and L. T. Huynh. Bifurcation analysis of Chua's Circuits. *Proc. of 35 th Midwest Symposium on Circuits and Systems*, pages 746–751, August 10-12, 1992. Washington D. C.

[23] R. Lozi and S. Ushiki. The theory of confinors in Chua's circuit: accurate analysis of bifurcations and attractors. *Int. J. of Bifurcation and chaos*, 3(2), April 1993.

[24] Lj. Kocarev, K.S. Halle, K. Eckert, L.O. Chua, and U. Parlitz. Experimental demonstration of secure communitions via chaotic synchronition. *Int. J. of Bifurcation and Chaos*, 2(3):709–713, Sept 1992.

[25] U. Parlitz, L.O. L. O. Chua, Lj. Kocarev, K. S. Halle, and A. Shang. Transmission of digital signals by chaotic synchronition. *Int. J. of Bifurcation and Chaos*, 2(4):973–977, Dec 1992.

[26] G. A. Johnson, T. E. Tigner, and E. R. Hunt. Controlling chaos in Chua's circuit. *J. of Circuits, Systems, Computers*, 3(1):109–117, March 1993.

[27] G. A. Johnson and E. R. Hunt. Mainining stability in Chua's circuit driven into regions of oscillation and chaos. *J. of Circuits, Systems and Computers*, 3(1), March 1993. 119-123.

[28] K. Murali and M. Lakshmanan. Controlling chaos in Chua's circuit. *J. of Circuits, Systems and Computers*, 3(1), March 1993. 125-137.

[29] Chen G.R. and Dong X.N. Controlling Chua's circuit. *J. of Circuits, Systems and Computers*, 3(1), March 1993. 139-149.

[30] R. Genesio and A. Tesi. Distortion control of chaotic systems. *J. of Circuits, Systems and Computers*, 3(1), March 1992. 61–79.

[31] T. Hartley and F. Mossayebi. Control of Chua's circuit. *J. of Circuits, Systems and Computers*, 3(1):173–194, March 1993.

[32] K.S. Halle, L.O. Chua, V.S. Anishchenko, and M.A. Safonova. Signals application via chaos. *Int. J. of Bifurcation and Chaos*, 2(4), Dec 1992. 1011-1020.

[33] M. Delgado Restituto and A. Rodriguez Vazquez. A CMOS monolithic Chua's circuit. *J. of Circuits, Systems and Computers*, 3(2), June 1993.

[34] J. H. Curry. A generalized Lorenz system. *Commun. Math. Phys.,*, 60:193–204, 1978.

[35] V. Franceschini and C. Boldrighini. A five-dimensional truncation of the plane incompressible Navier-Stokes equations. *Commun. Math. Phys.,*, 64:159–170, 1979.

[36] V. Franceschini and C. Tebaldi. Sequences of infinite bifurcations and turbulence in a 5-mode truncation of the Navier-Stokes equations. *J. Stat. Phys.,*, 21:707–726, 1979.

[37] V. Franceschini and C. Tebaldi. A 7-mode truncation of the Navier-Stokes equations. *Preprint, University di Modena, Italy*, 1980.

[38] J. D. Gibbon and M. J. McGuinness. The real and comlplex Lorenz equations in rotating fluids and lasers. *Physica D*, 1993.

[39] V. Perez-Munuzuri, V. Perez-Villar, and L.O. Chua. Autowaves for image processing on a 2-dimensional CNN array of Chua's circuits. *IEEE Trans CAS*, 40(3), March 1993.

[40] Lj. Kocarev, Lj. Karadzinov, and L. O. Chua. N-dimensional canonical Chua's circuit. *J. of Circuits, Systems and Computers*, 3(1):239–258, March 1993.

[41] K.A Lukin. High frequency oscillation from Chua's circuit. *J. of Circuits, Systems and Computers*, 3(2), June 1993.

[42] A.N. Sharkovsky, Yu. Maistrenko, P. Deregel, and L.O. Chua. Dry turbulence from a time-delayed Chua's circuit. *J. of Circuits, Systems and Computers*, 3(2), June 1993.

[43] T. L. Carroll and L. M. Pecora. A circuit for studying the synchronization of chaotic sytems. *Int. J. of Bifurcation and Chaos*, 2(3):659–667, 1992.

Figure Captions

Fig.1. Lorenz attractor
(a) 3-D phase portrait
(b) Projection of the attractor onto the (x,z) plane
(c) Waveform of $x(t)$

Fig.2. Chua's circuit consisting of 4 linear elements and a nonlinear resistor N_R
(a) Chua's circuit
(b) The $v - i$ characteristic of the nonlinear resistor (Chua's diode)

Fig.3. Double-scroll Chua's attractor
(a) 3-D phase portrait
(b) Projection of the attractor onto the (x,z) plane
(c) Waveform of $x(t)$

Fig.4. (a) Equilibrium points in Lorenz equation and their associated eigenvalue configurations.
(b) A schematic view of the flow near equilibrium points.

Fig.5. (a) Equilibrium points in Chua's equation and their associated eigenvalue configurations.
(b) A schmatic view of the flow near equilibrium points.

Fig.6. Homoclinic orbit of the origin in Lorenz equation

Fig.7. Homoclinic orbit of the origin in Chua's equation

Fig.8. Period-doubling phenomenon in Lorenz equation
(a) period-3 orbit ($r = 100.5$)
(b) period-6 orbit ($r = 99.96$)
(c) period-12 orbit ($r = 99.6$)
(d) chaotic attractor ($r = 99.4$)

Fig.9. Period-doubling phenomenon in Chua's equation
(a) period-1 orbit ($\alpha = 8.8, \beta = 16$)
(b) period-2 orbit ($\alpha = 8.86, \beta = 16$)
(c) period-4 orbit ($\alpha = 9.12, \beta = 16$)
(d) chaotic attractor ($\alpha = 9.4, \beta = 16$)

Fig.10. Intermittent chaos in Lorenz equation

Fig.11. Intermittent chaos in Chua's equation

Fig.12. Meta-stable chaos in Lorenz equation. A typical trajectory wanders chaotically near a strange set before it is attracted to a fixed point.

Fig.13. Meta-stable chaos in Chua's equation. A typical tractory wanders chaotically near a strange set before it is attracted to a stable periodic orbit.

Fig.14. (a) Semi-periodicity in Lorenz equation
(b) The Poincare cross section at $x = 20$.

Fig.15. (a) Semi-periodicity in Chua's equation
(b) The Poincare cross section at $x = 1$.

Fig.16. Two co-existing chaotic attractors (a) and (b) in the Lorenz equation

Fig.17. Three co-existing chaotic attractors (a), (b) and (c) in the Chua's equation

Fig.18. Afraimovich-Bykov-Shil'mkov geometric model
(a) A box around the origin and two tubes surrounding the two branches of the unstable

manifold of the origin

(b) The two-dimensional map T. The maps in A, B and C correspond to the orientable, semiorientable and nonorientable cases, respectively.

Fig.19. Template for the Lorenz attractor

Fig.20. Belykh-Chua geometric model

(a) A cylinder G around the origin and two tubes surrounding the unstable manifold of the origin. The return points P_1 and P_2 are drawn for the case $\mu = 0$.

(b) The two-dimensional map f. The image of the upper or lower half portion of the disks d_1 and d_2 gives rise to Shil'nikov snakes: $d_{ij} = f_i(D_i \cap d_j)$, $i,j = 1,2$, where $f_i = f|_{D_i}$.

Fig.21. Induced template for the double-scroll Chua's attractor

Fig.22. Two distinct chaotic attractors from the Lorenz equation

(a) $\sigma = 10$, $b = 2.667$, $\gamma = 28$

(b) $\sigma = 10$, $b = 0.25$, $\gamma = 490$

Fig.23. Six distinct non-periodic attractors from the Chua's equation

(a) $\alpha = 9.4$, $\beta = 16$, $a = -1.1428$, $b = -0.7143$

(b) $\alpha = 1800$, $\beta = 10000$, $a = -1.026$, $b = -0.982$

(c) $\alpha = 9$, $\beta = 14.2857$, $a = -1.1428$, $b = -0.7143$

(d) $\alpha = 8.342$, $\beta = 11.925$, $a = -0.7048$, $b = -1.146$

(e) $\alpha = -4.925$, $\beta = -3.649$, $a = -2.497$, $b = -0.9301$

(f) $\alpha = -4.087$, $\beta = -2.0$, $a = -1.1429$, $b = -0.7142$

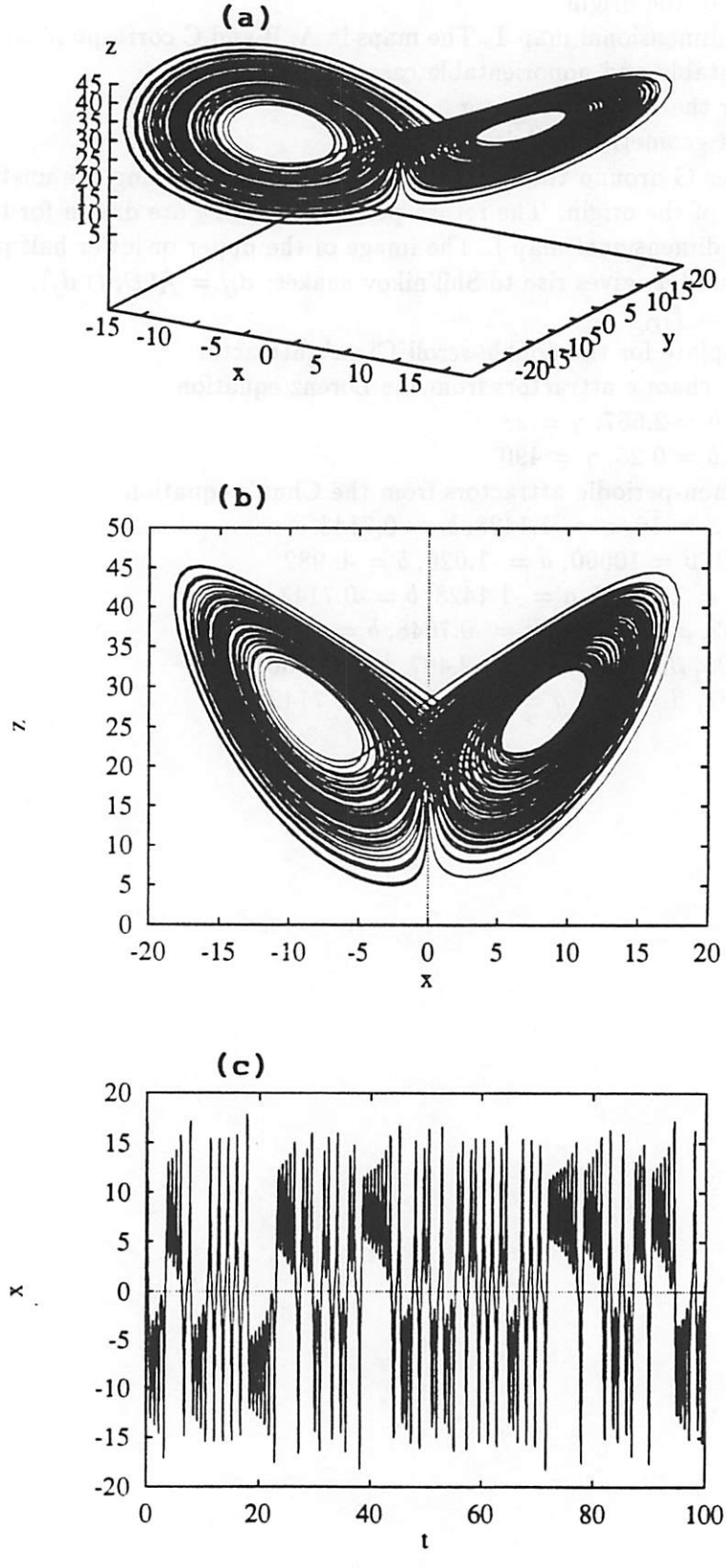
(a)
z
x
y
(b)
z
x
(c)
x
t

Fig. 2

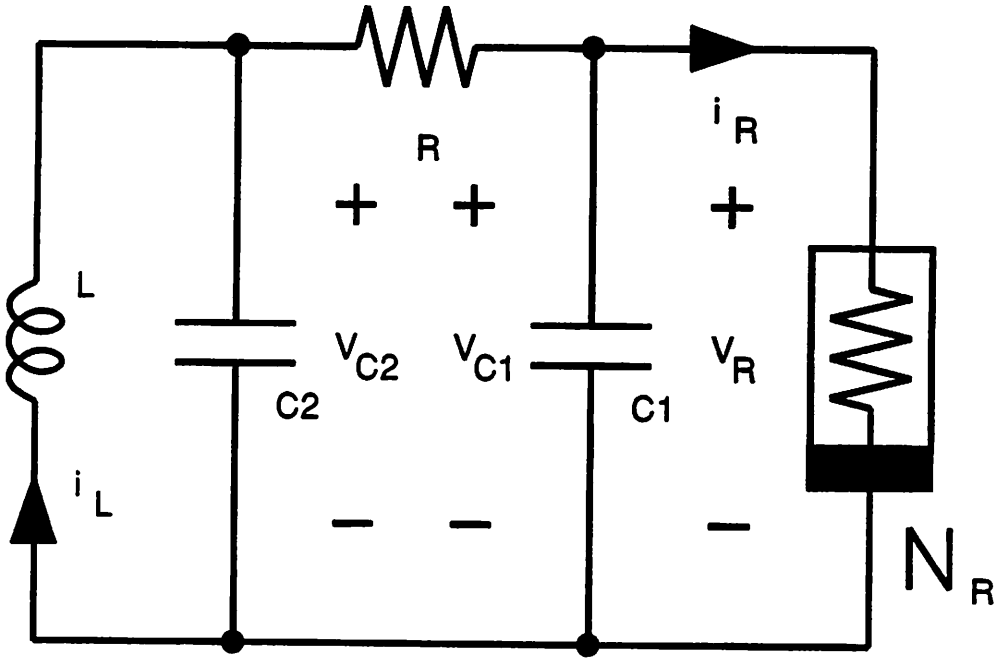

Fig.2

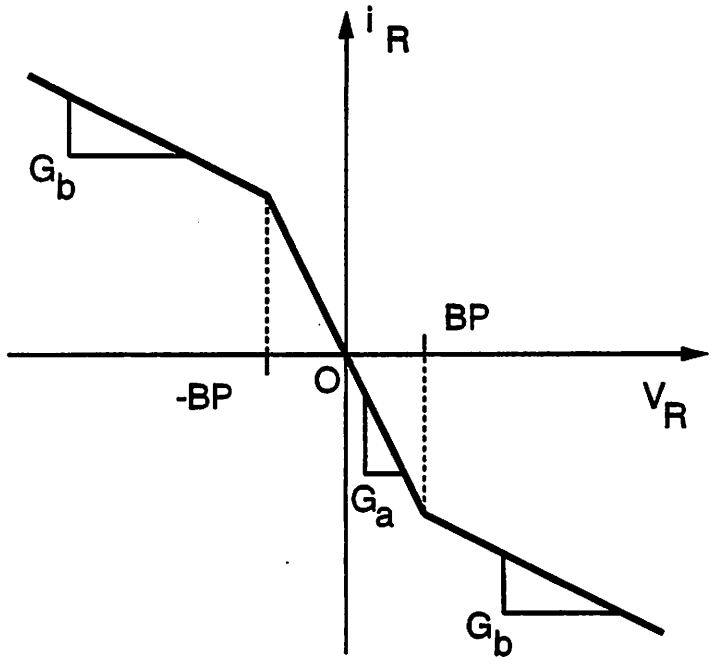

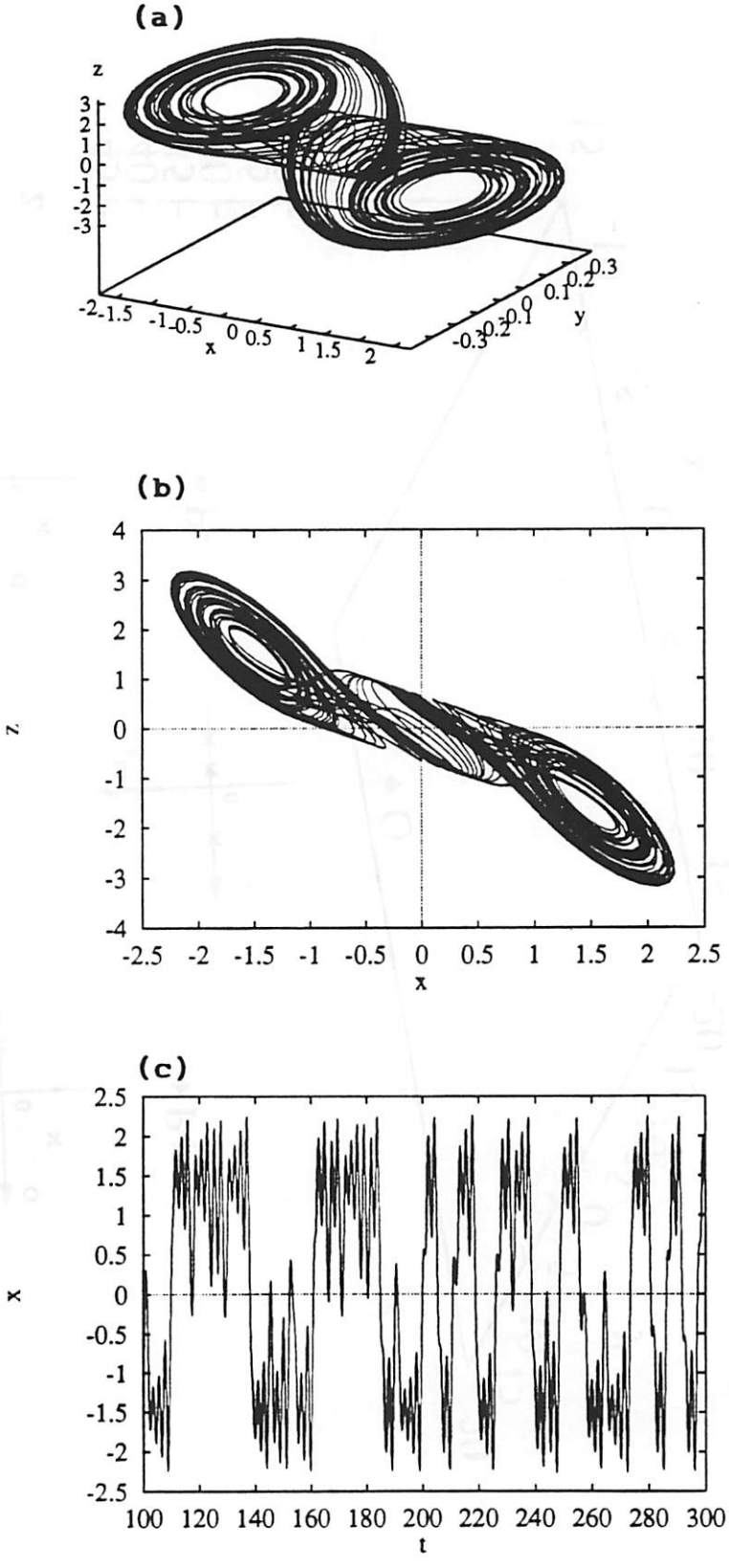
(a)
z
3
2
1
0
-1
-2
-3
-2 -1.5 -1 -0.5 0 0.5 1 1.5 2
x
-0.3 -0.2 -0.1 0 0.1 0.2 0.3
y
(b)
z
4
3
2
1
0
-1
-2
-3
-4
-2.5 -2 -1.5 -1 -0.5 0 0.5 1 1.5 2 2.5
x
(c)
x
2.5
2
1.5
1
0.5
0
-0.5
-1
-1.5
-2
-2.5
100 120 140 160 180 200 220 240 260 280 300
t

Fig. 4a

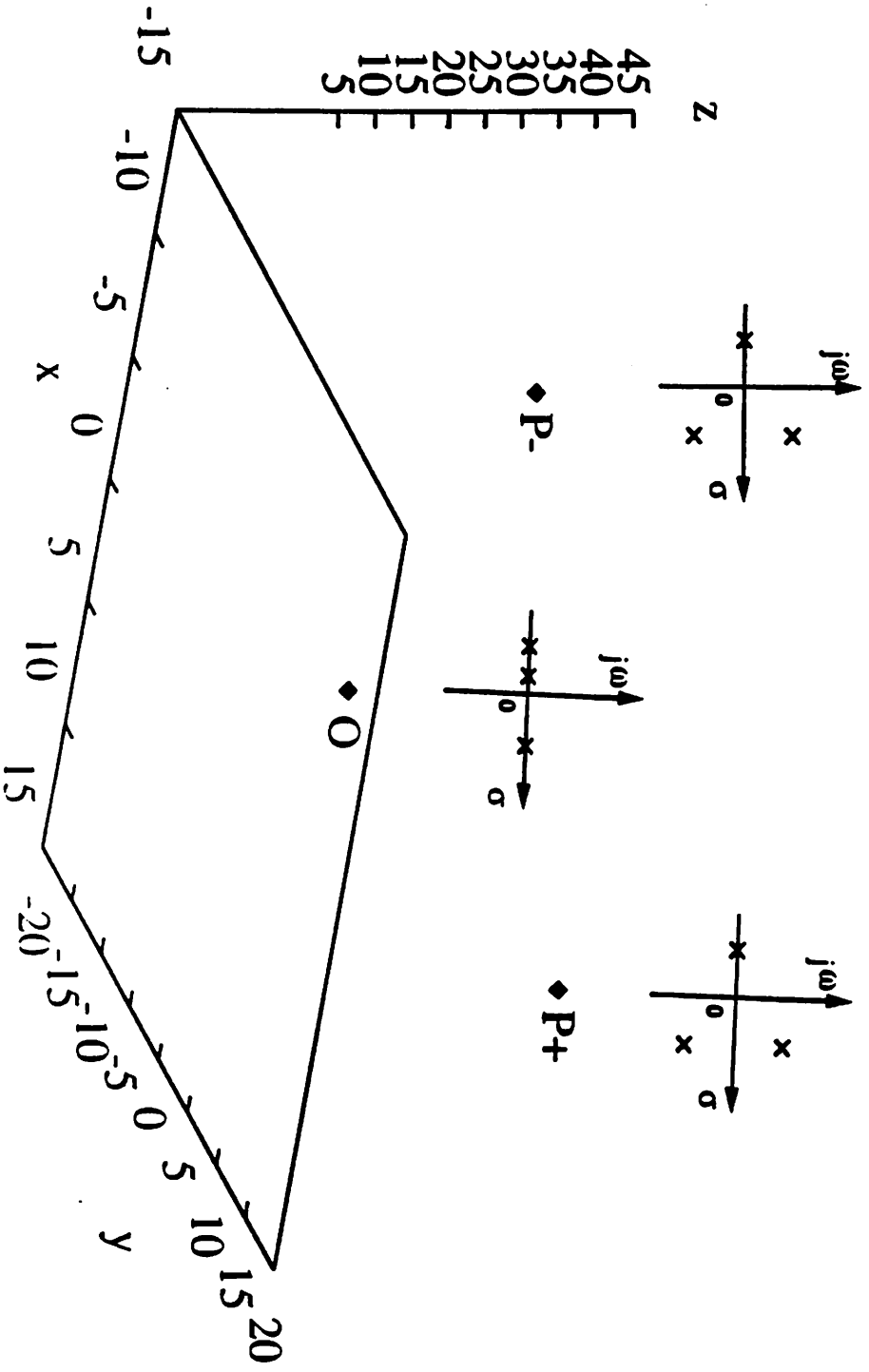
z
45
40
35
30
25
20
15
10
5
-15
-10
-5
0
5
10
15
x
-20
-15
-10
-5
0
5
10
15
20
y
O
P-
P+
jω
σ

Fig. 4 (6

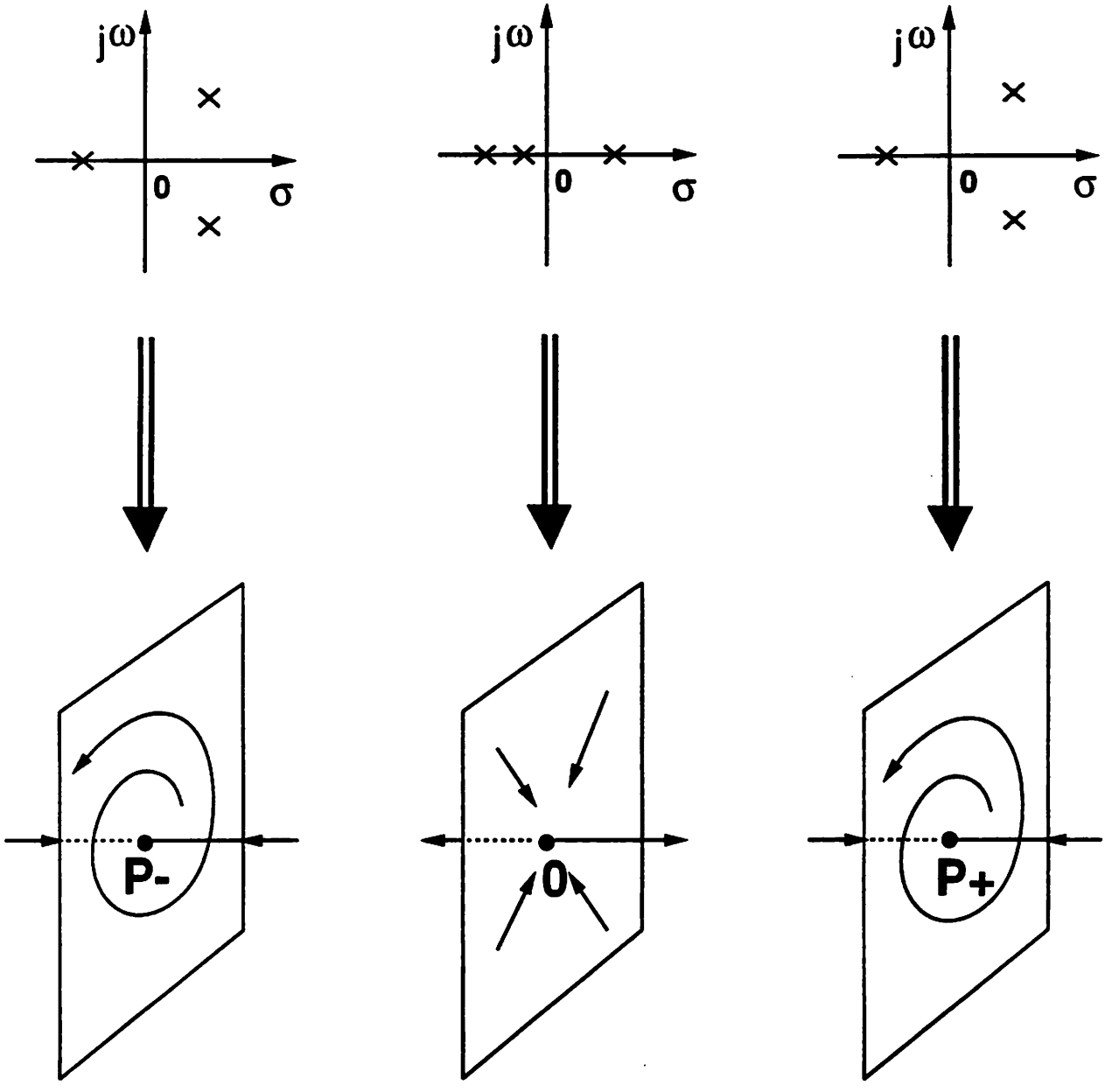

Fig. 5(a)

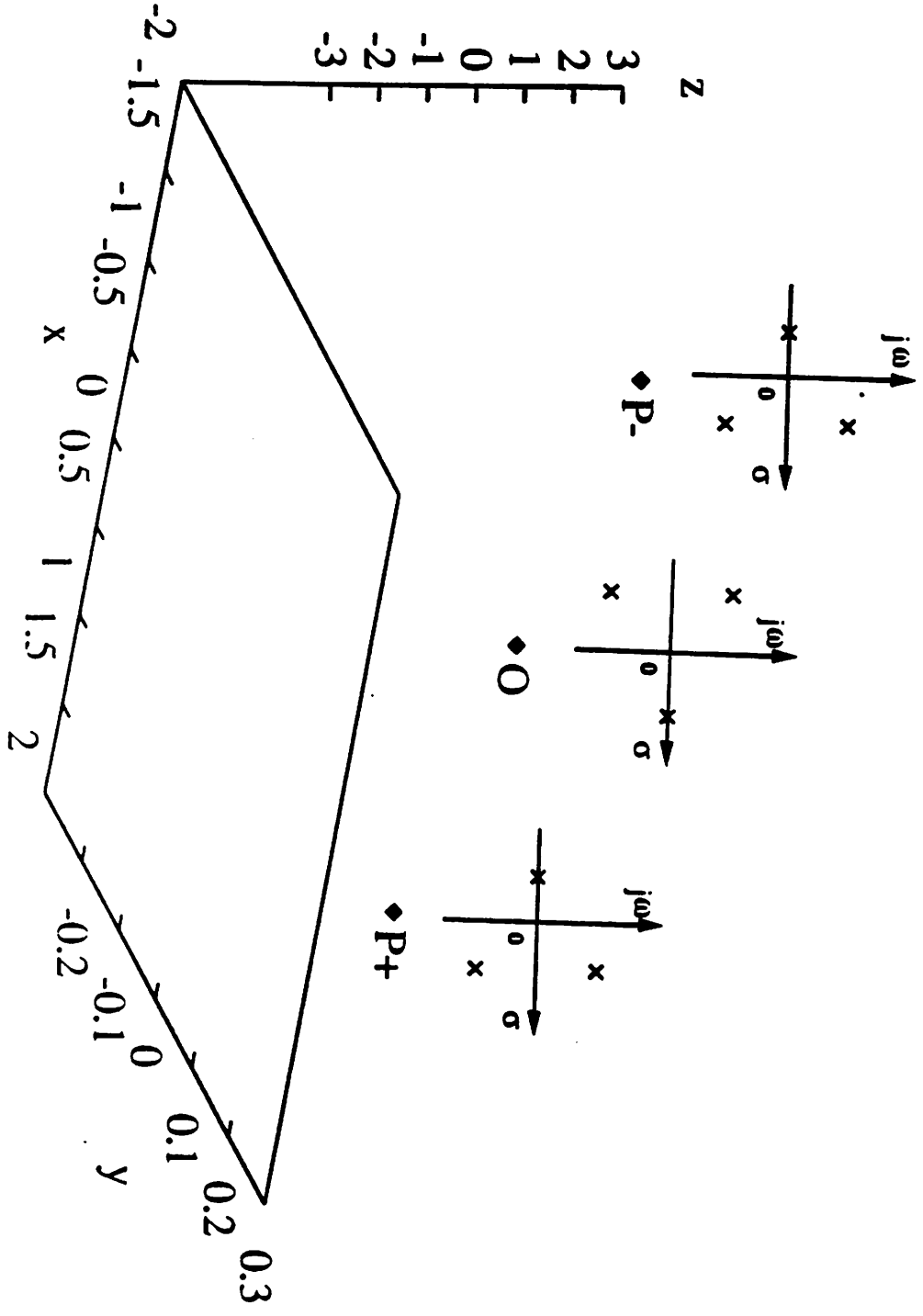

Fig. 5 (6)

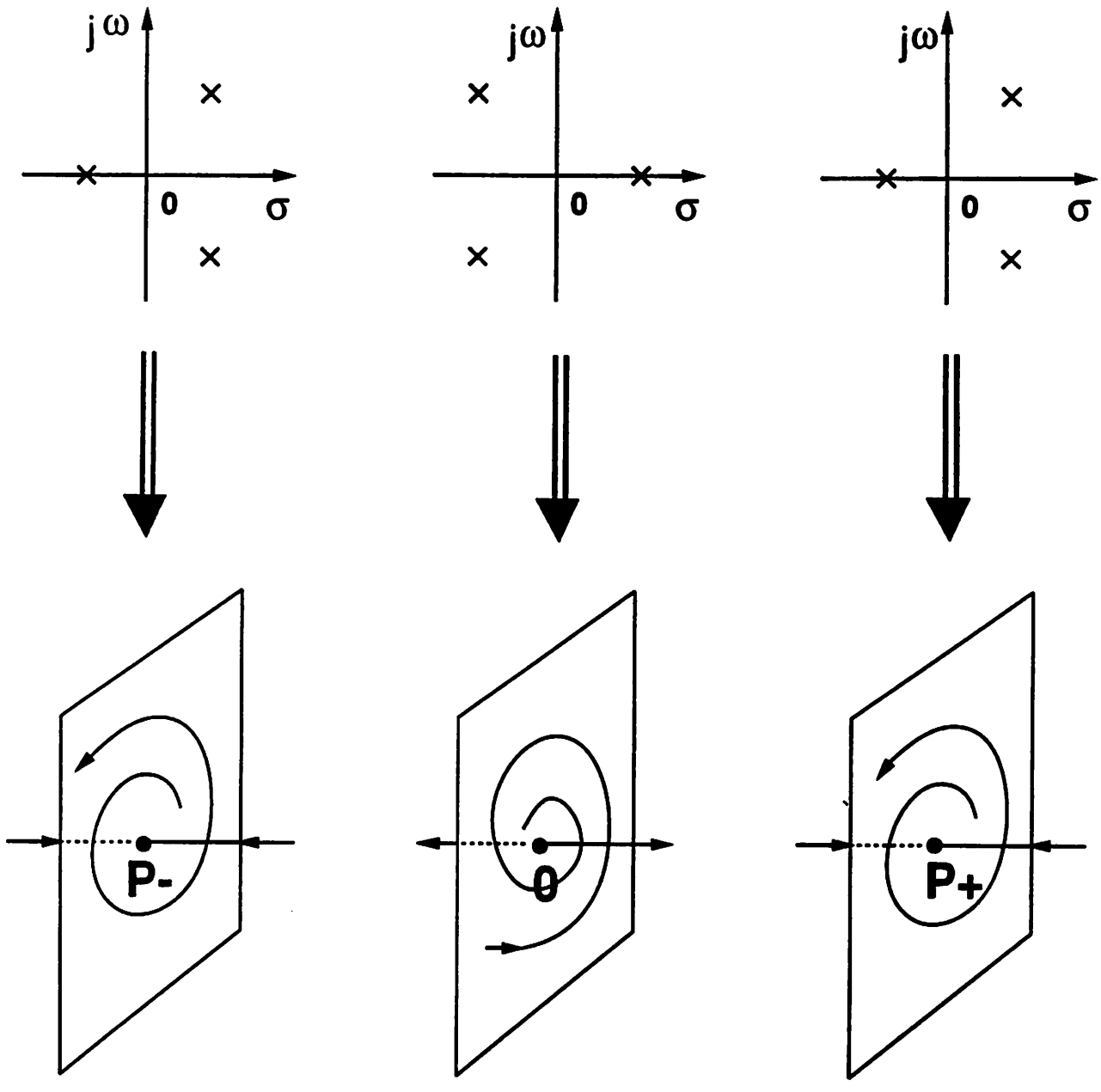

Fig. 6

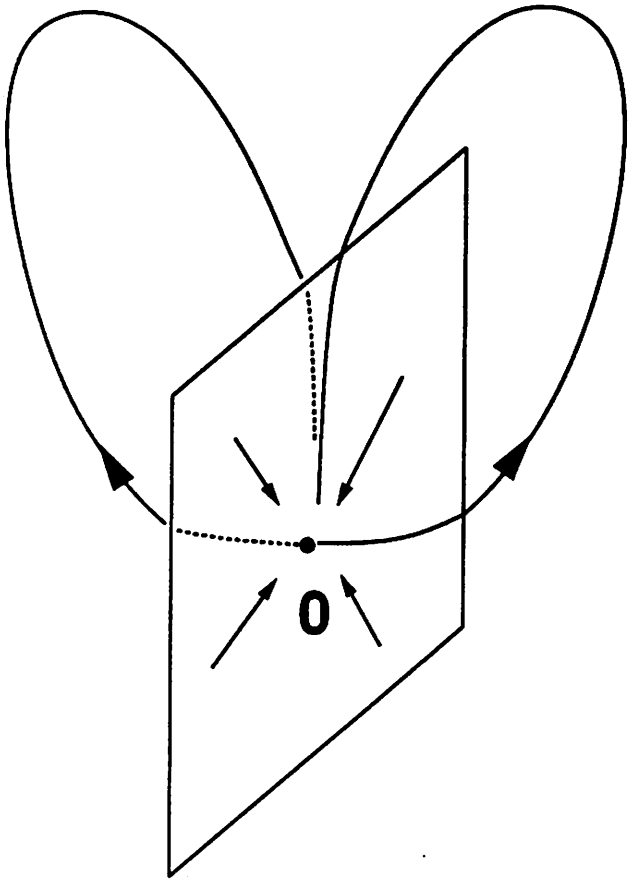

Fig 7

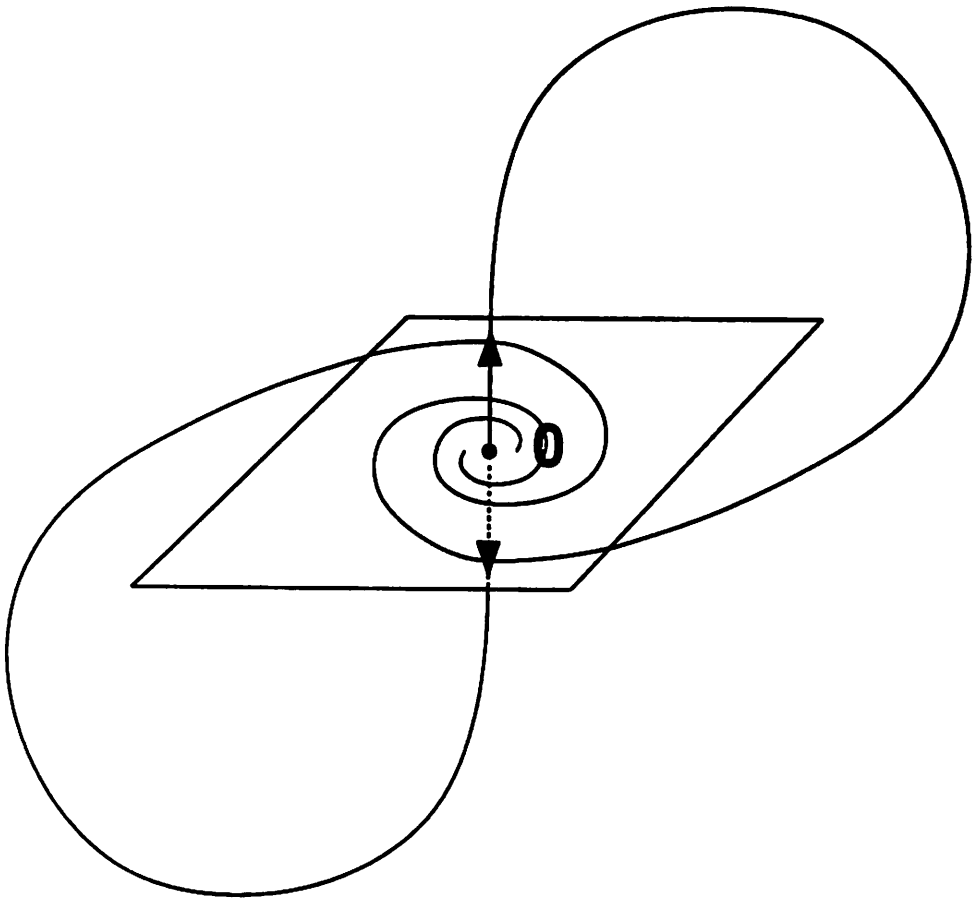

Fig .

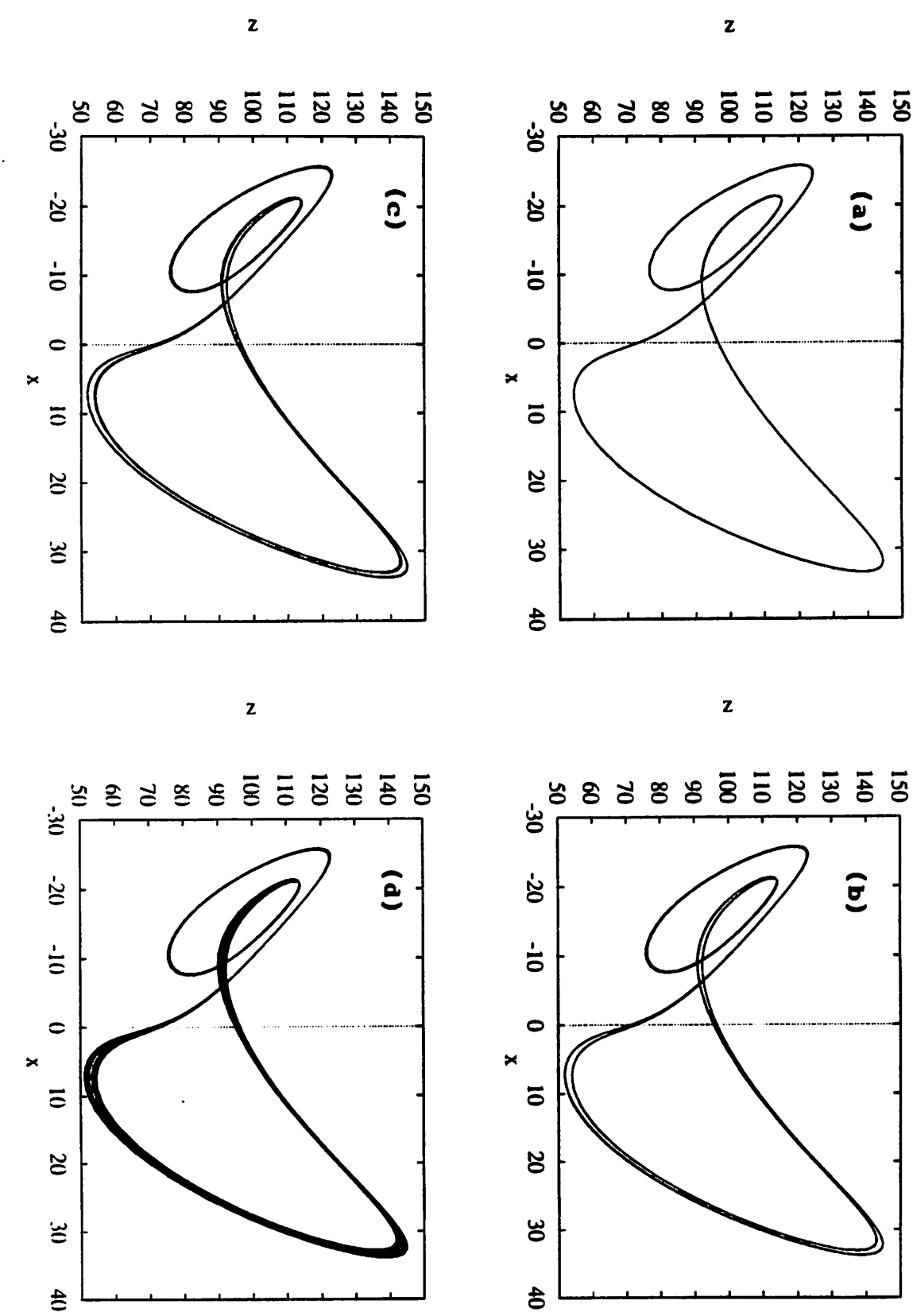

Fig.

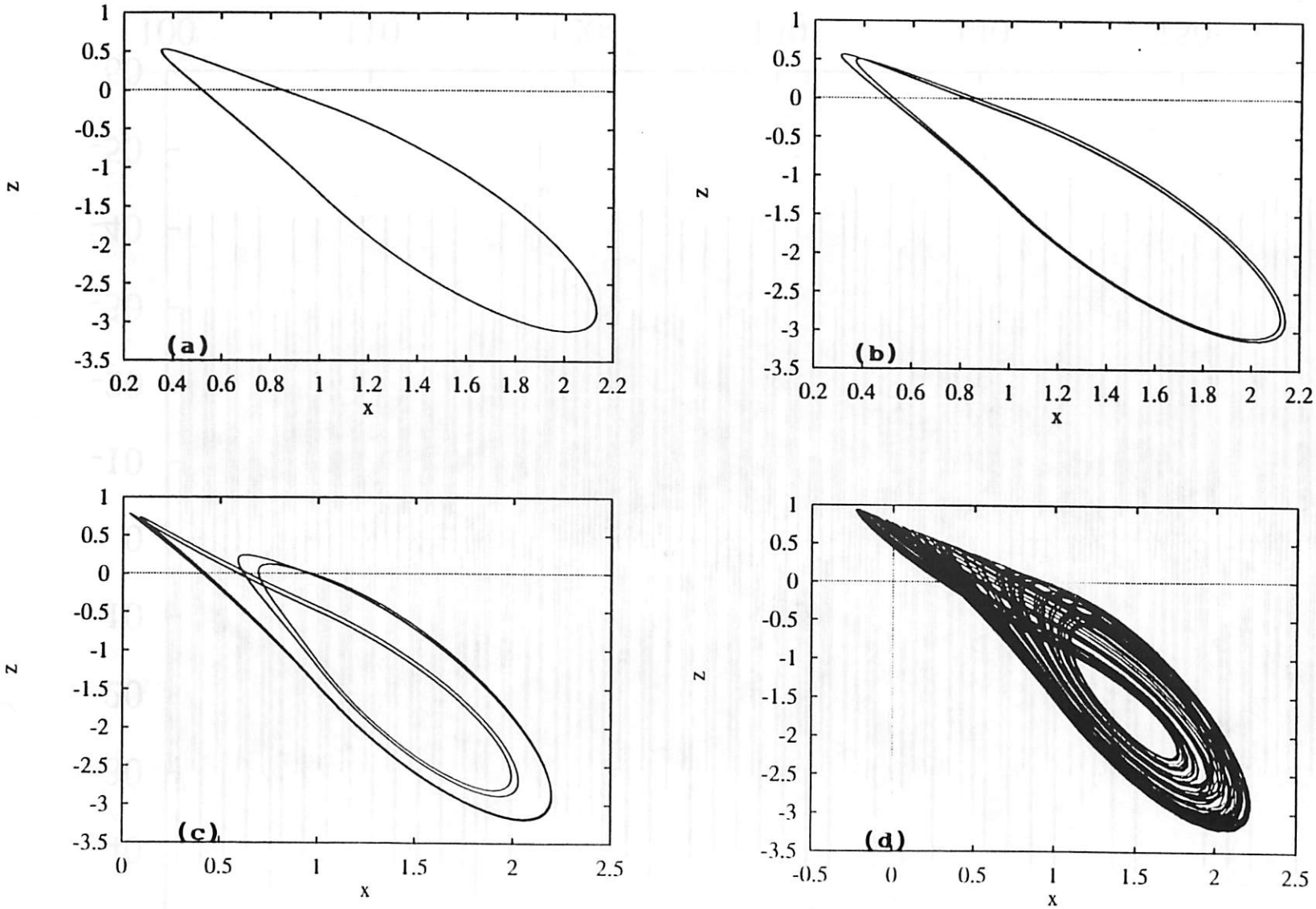

Fig. 10

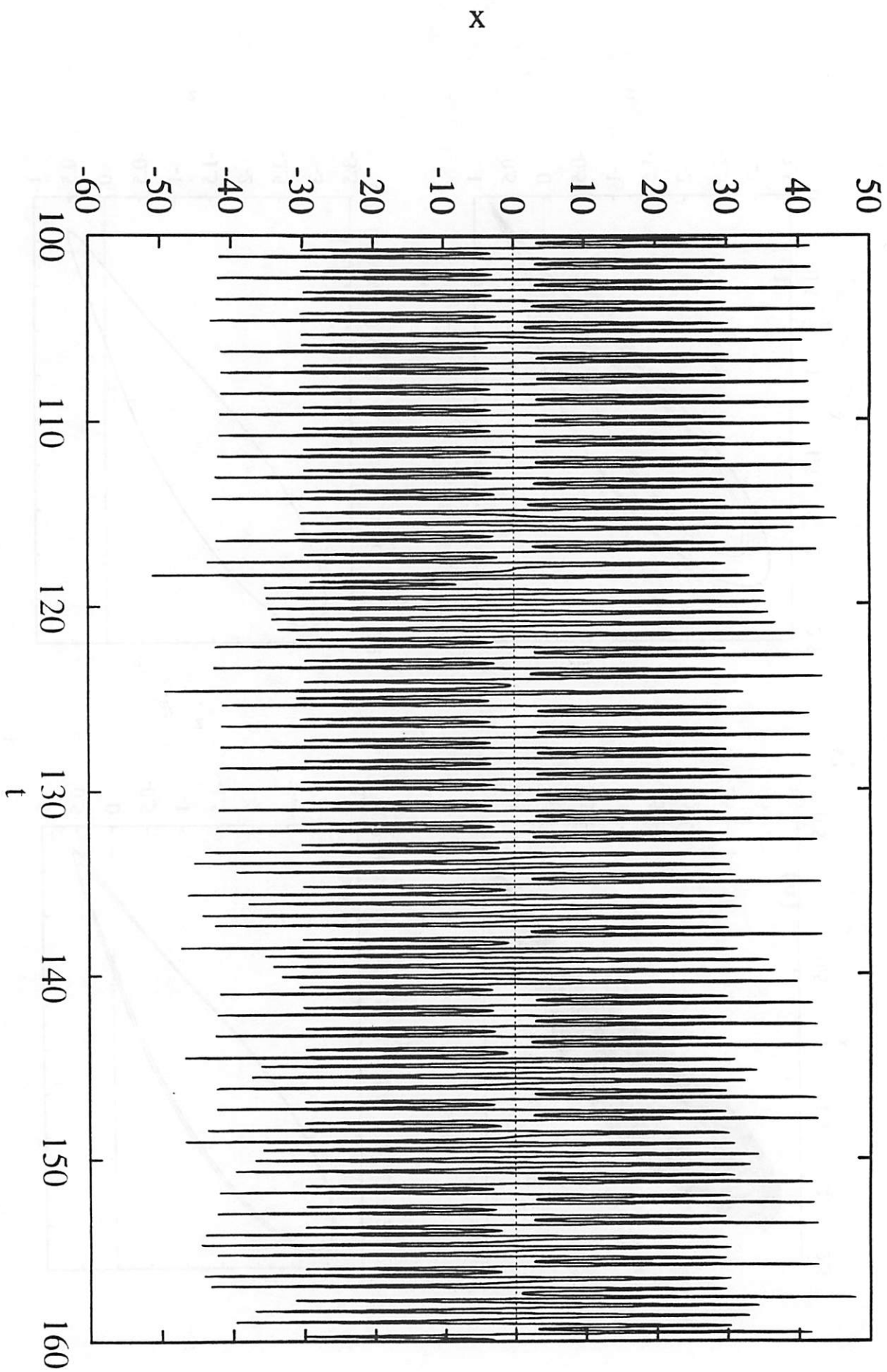

Fig. 11

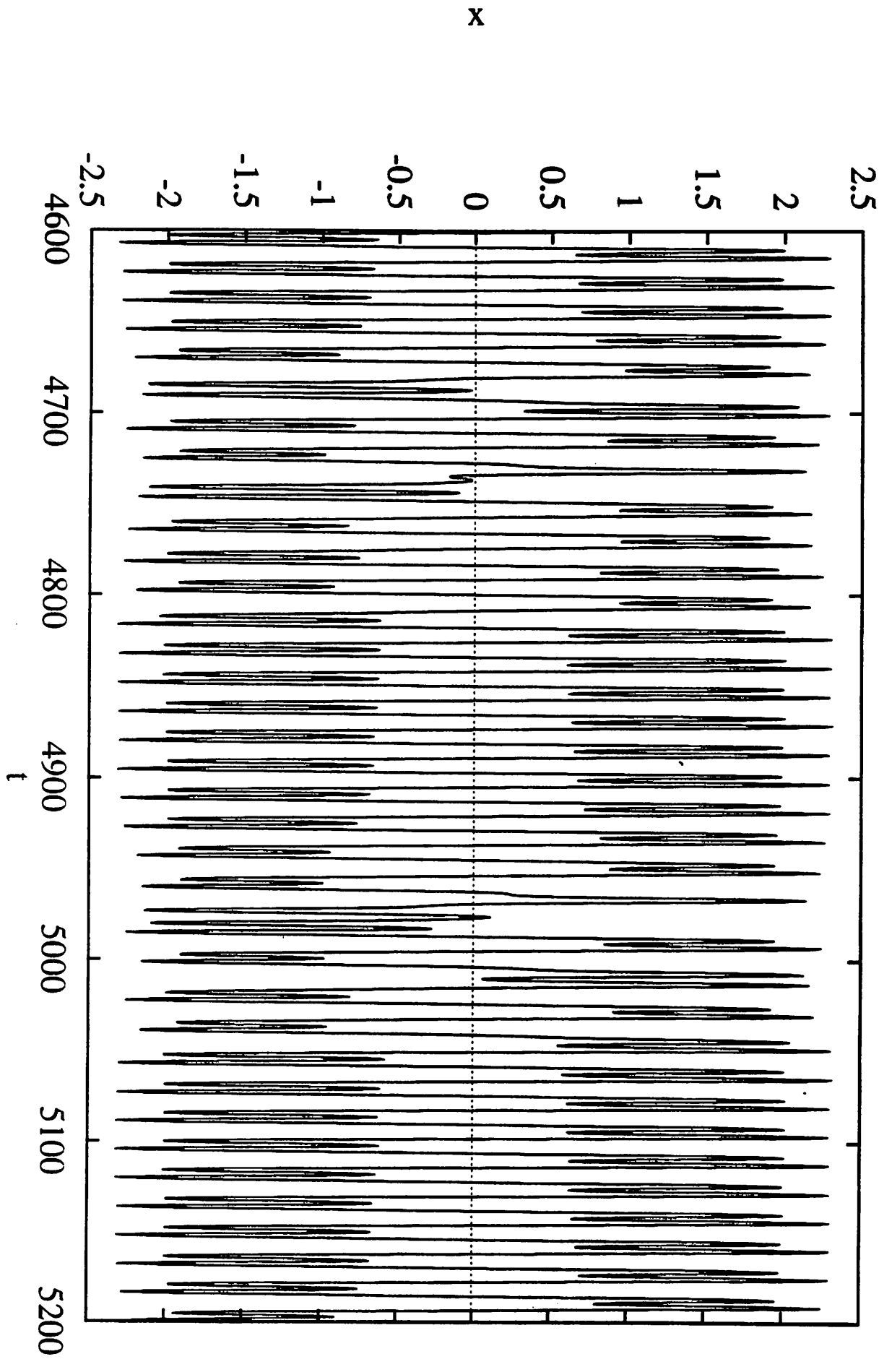

Fig. 1

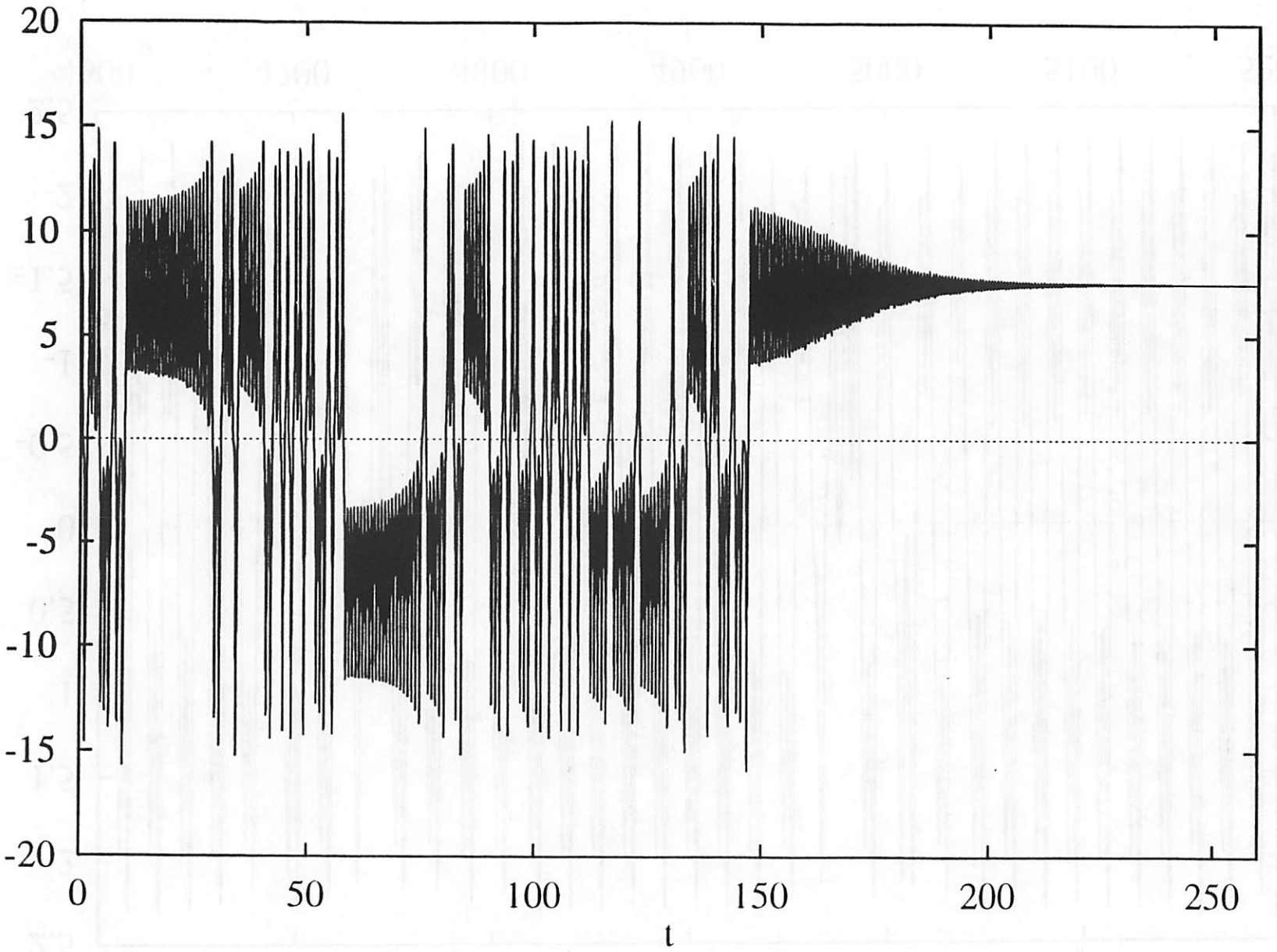

Fig. 13

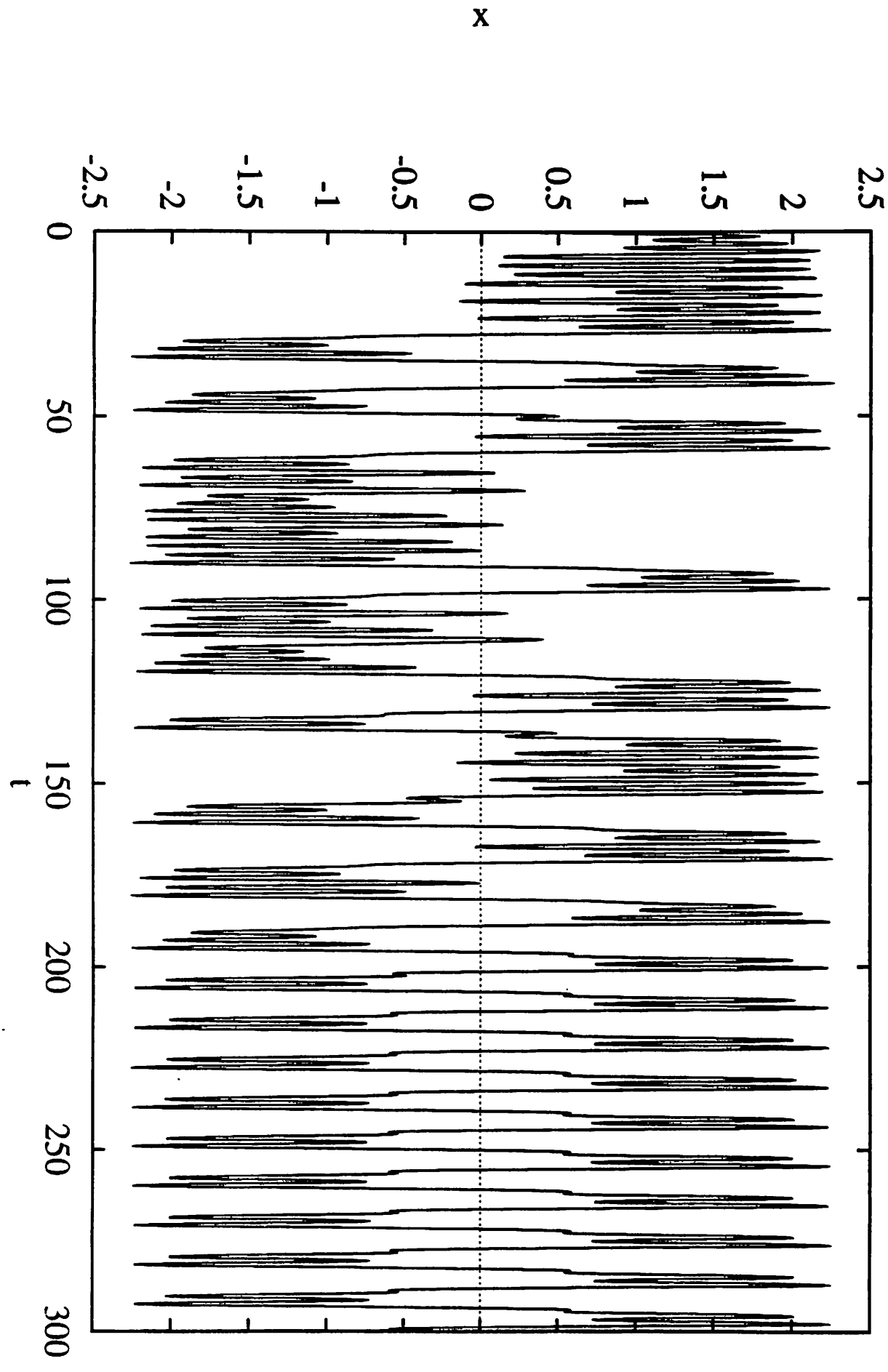

Fig

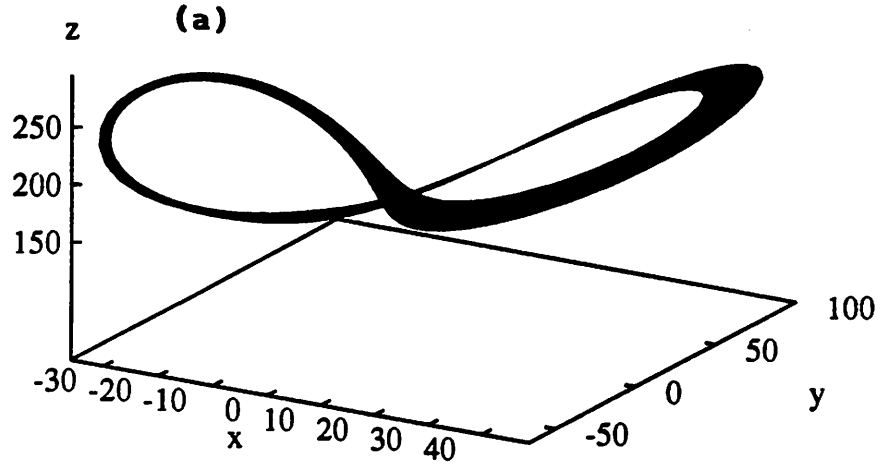
(a)
z
250
200
150
-30
-20
-10
0
10
20
30
40
x
100
50
0
-50
y

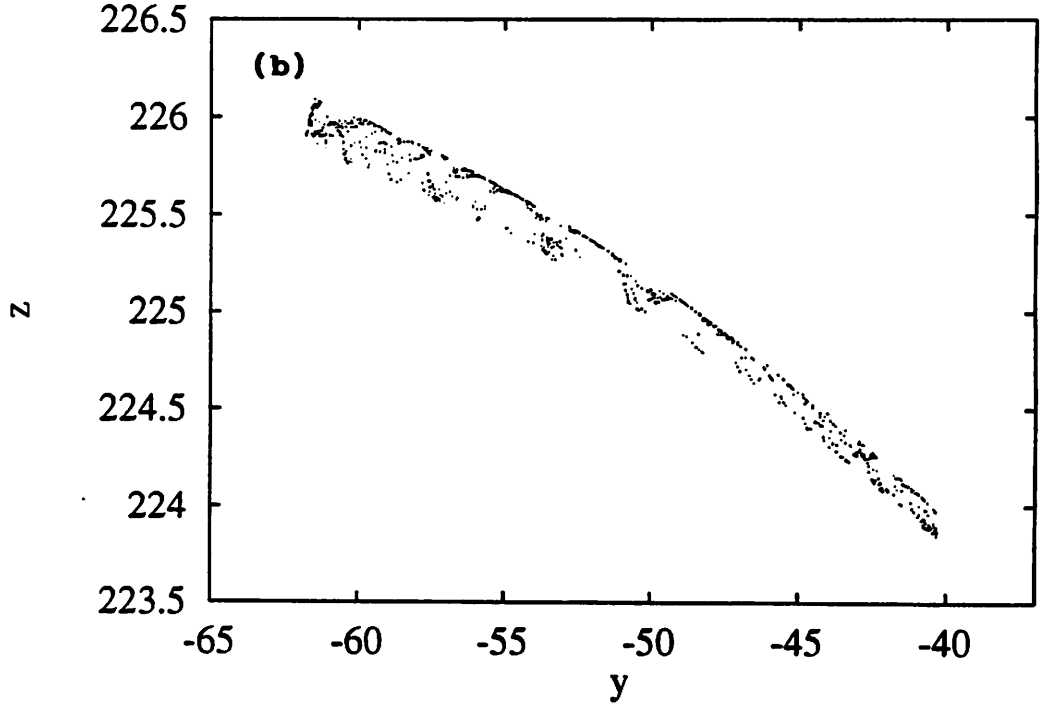
(b)
226.5
226
225.5
225
224.5
224
223.5
z
-65
-60
-55
-50
-45
-40
y

Fig.

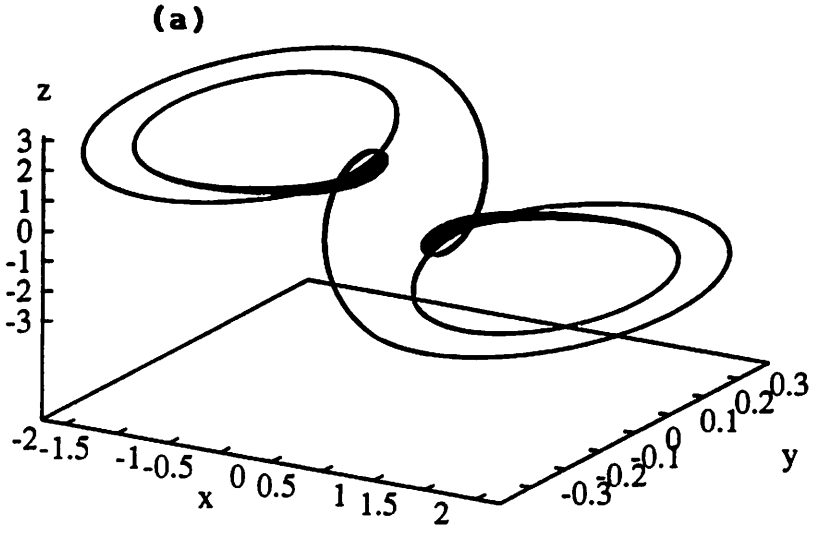
(a)
z
3
2
1
0
-1
-2
-3
-2
-1.5
-1
-0.5
0
0.5
1
1.5
2
x
-0.3
-0.2
-0.1
0
0.1
0.2
0.3
y

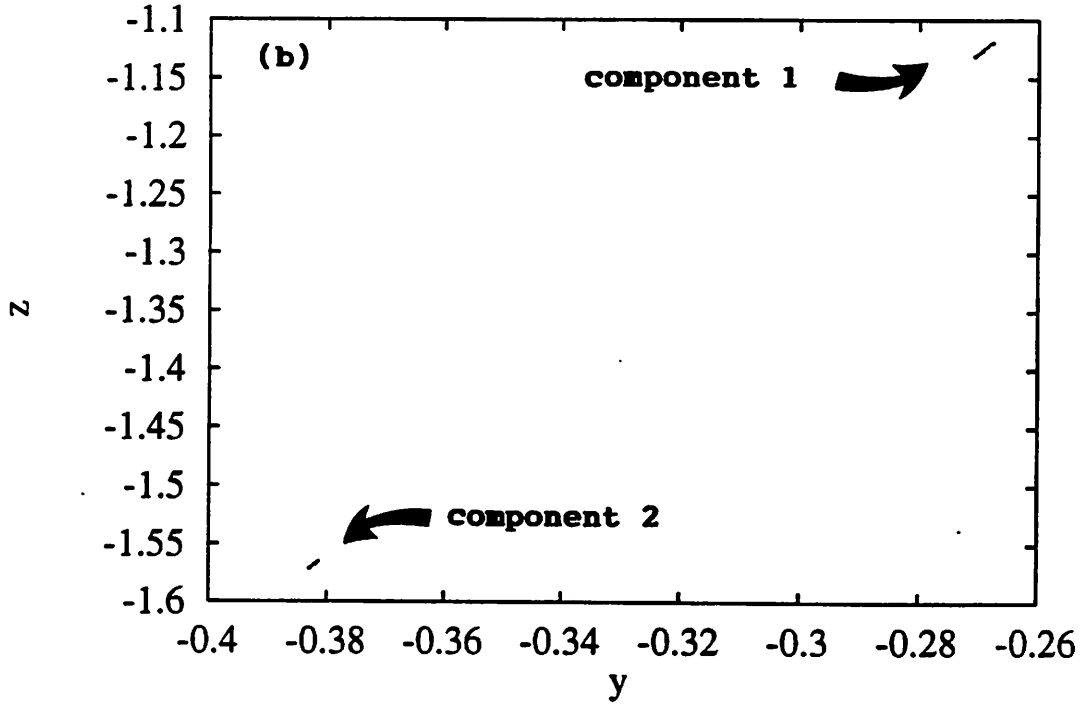
(b)
component 1
component 2
z
-1.1
-1.15
-1.2
-1.25
-1.3
-1.35
-1.4
-1.45
-1.5
-1.55
-1.6
-0.4
-0.38
-0.36
-0.34
-0.32
-0.3
-0.28
-0.26
y

Fig. 1e

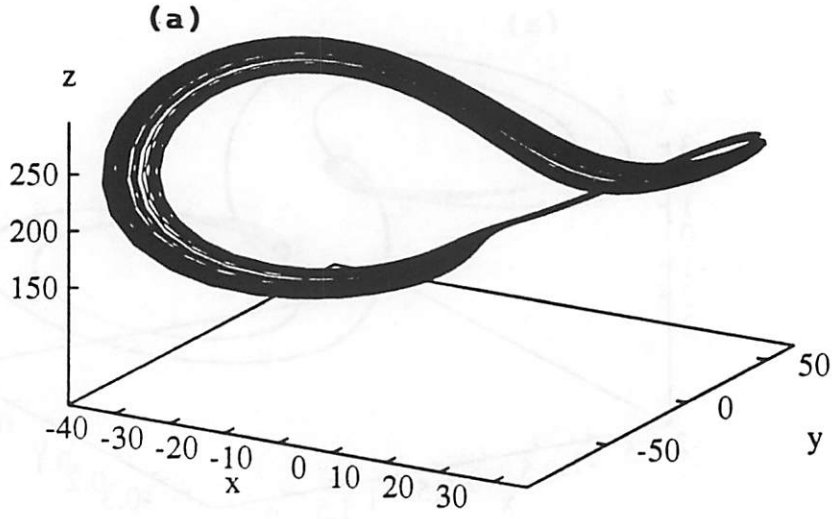
(a)
z
250
200
150
-40 -30 -20 -10 0 10 20 30
x
50
0
-50
y

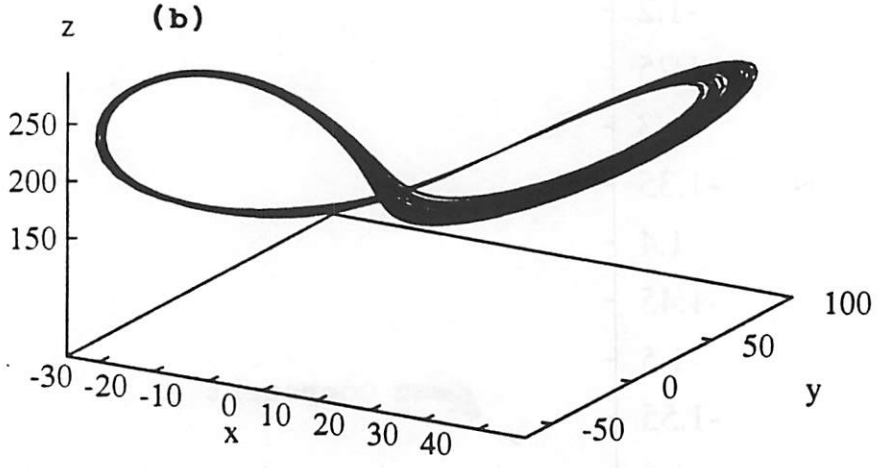
(b)
z
250
200
150
-30 -20 -10 0 10 20 30 40
x
100
50
0
-50
y

Fig.

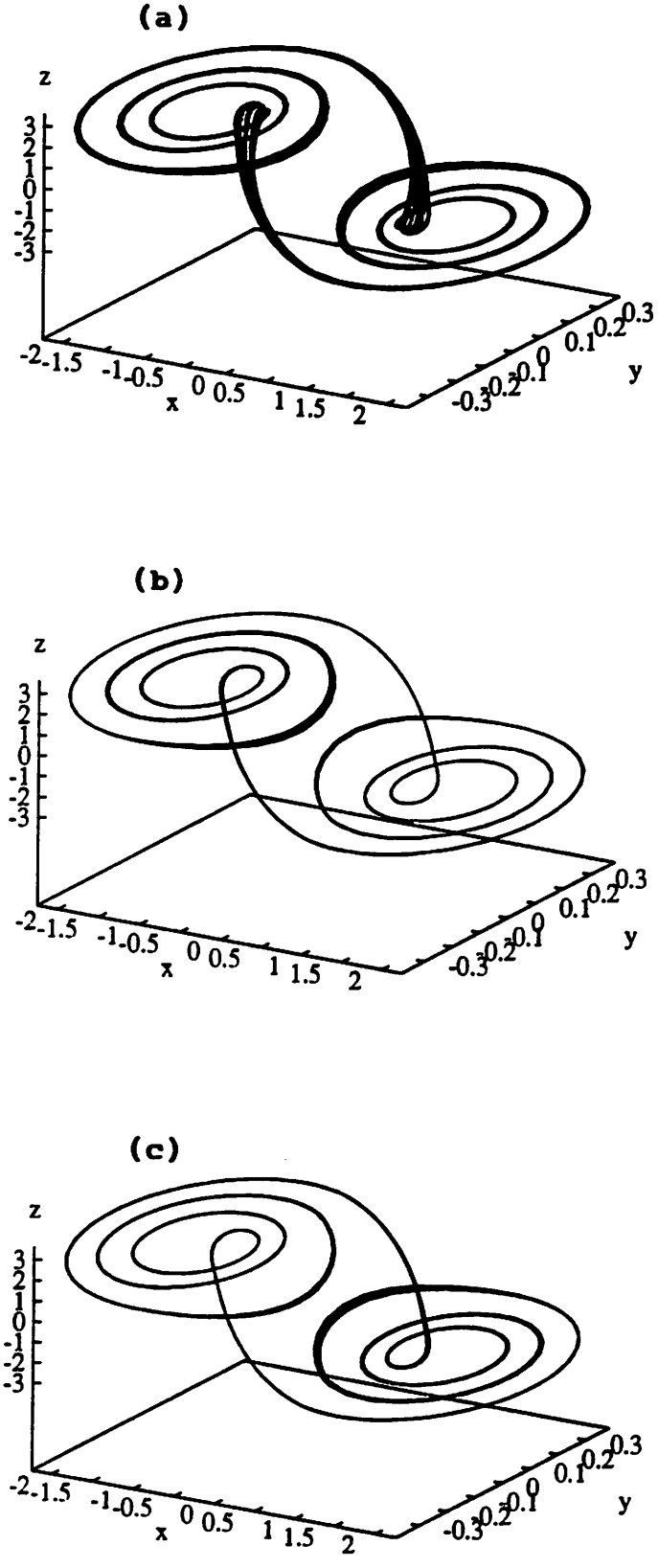
(a)
z
3
2
1
0
-1
-2
-3
-2 -1.5 -1 -0.5 0 0.5 1 1.5 2
x
-0.3 -0.2 -0.1 0 0.1 0.2 0.3
y
(b)
z
3
2
1
0
-1
-2
-3
-2 -1.5 -1 -0.5 0 0.5 1 1.5 2
x
-0.3 -0.2 -0.1 0 0.1 0.2 0.3
y
(c)
z
3
2
1
0
-1
-2
-3
-2 -1.5 -1 -0.5 0 0.5 1 1.5 2
x
-0.3 -0.2 -0.1 0 0.1 0.2 0.3
y

Fig. 18/1

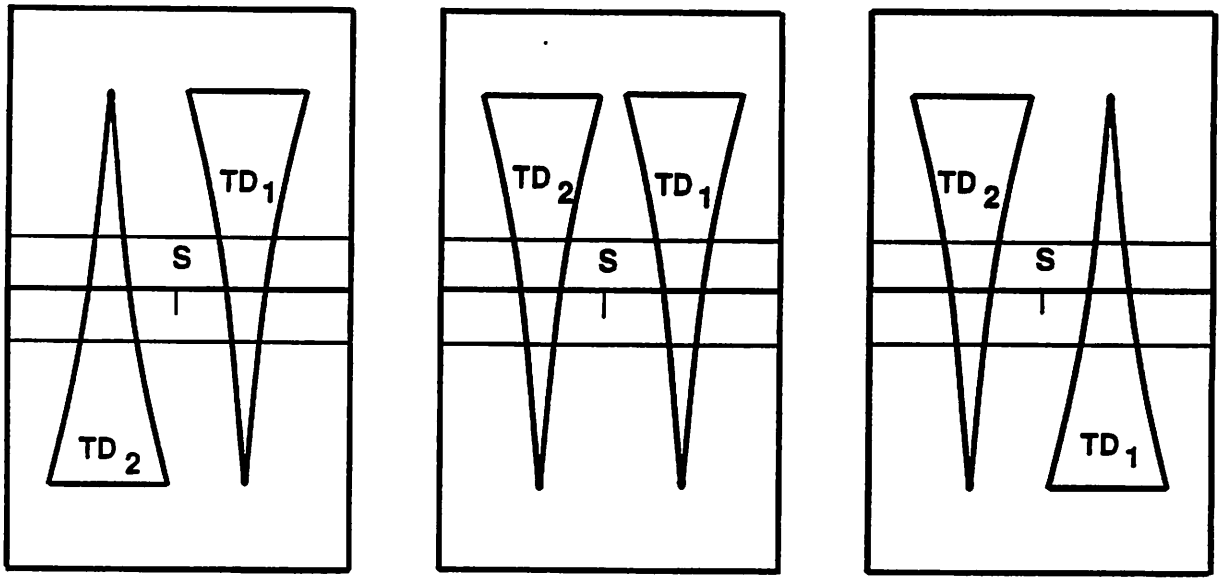

Fig. 18

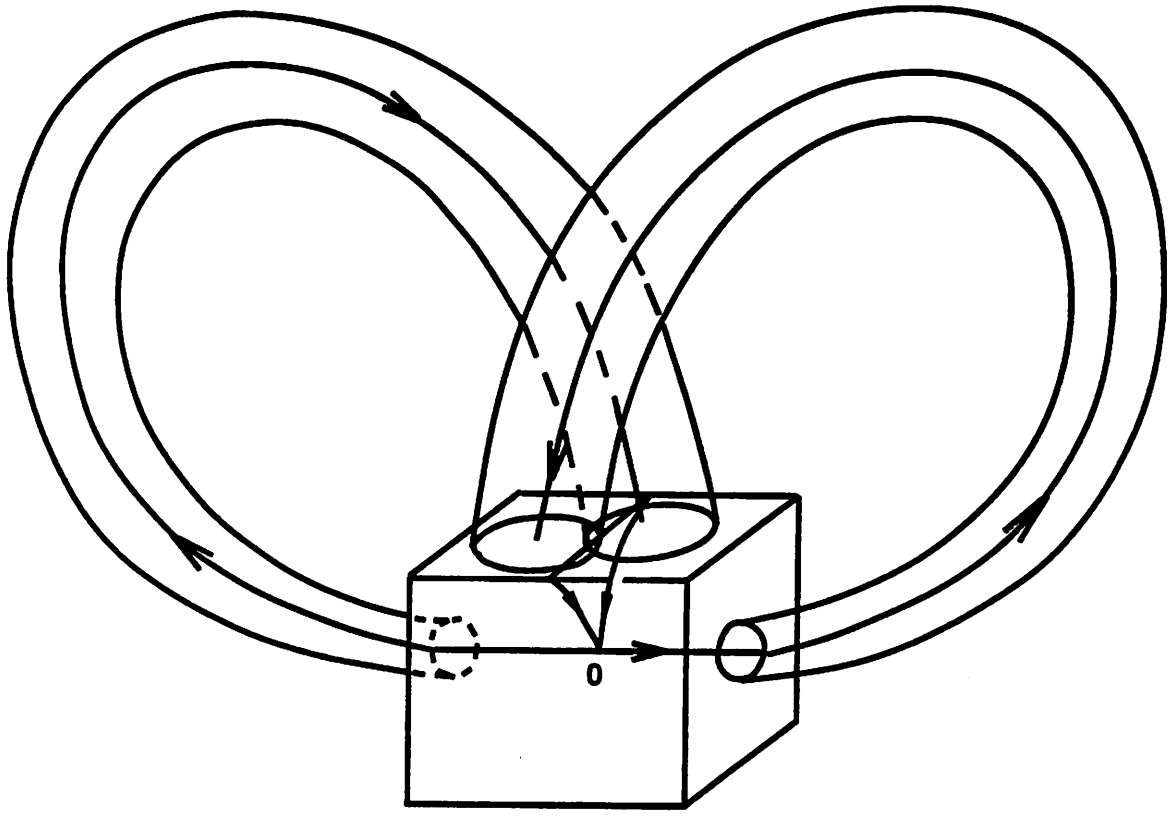

Fig. 1c

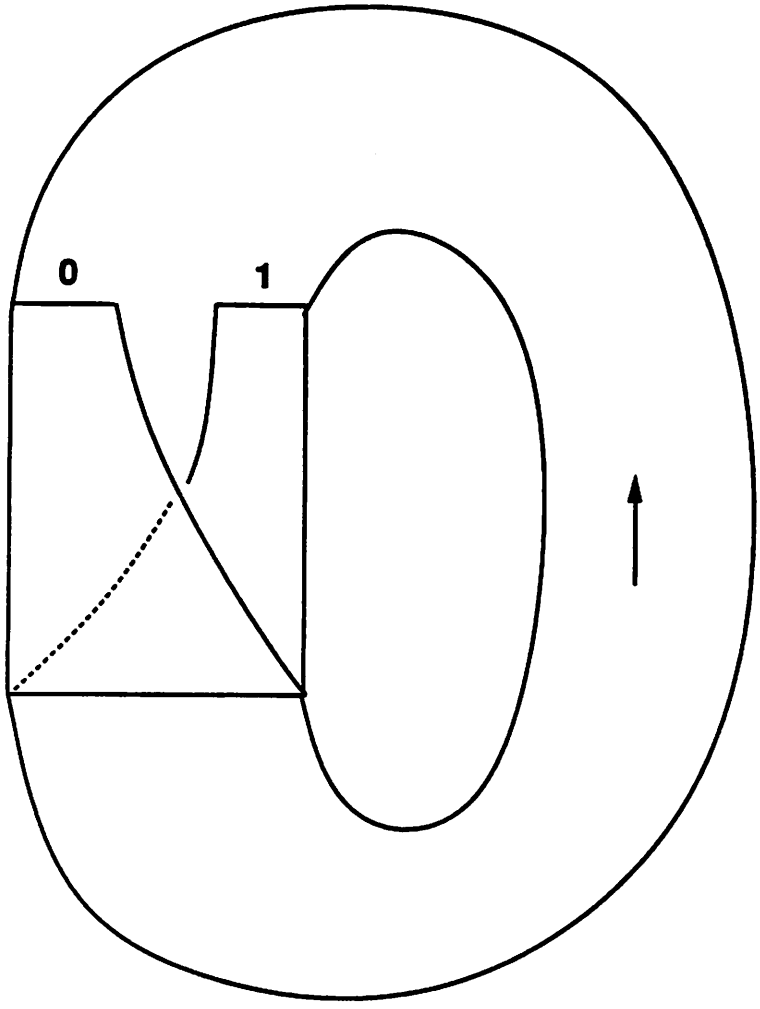

Fig. 20(a)

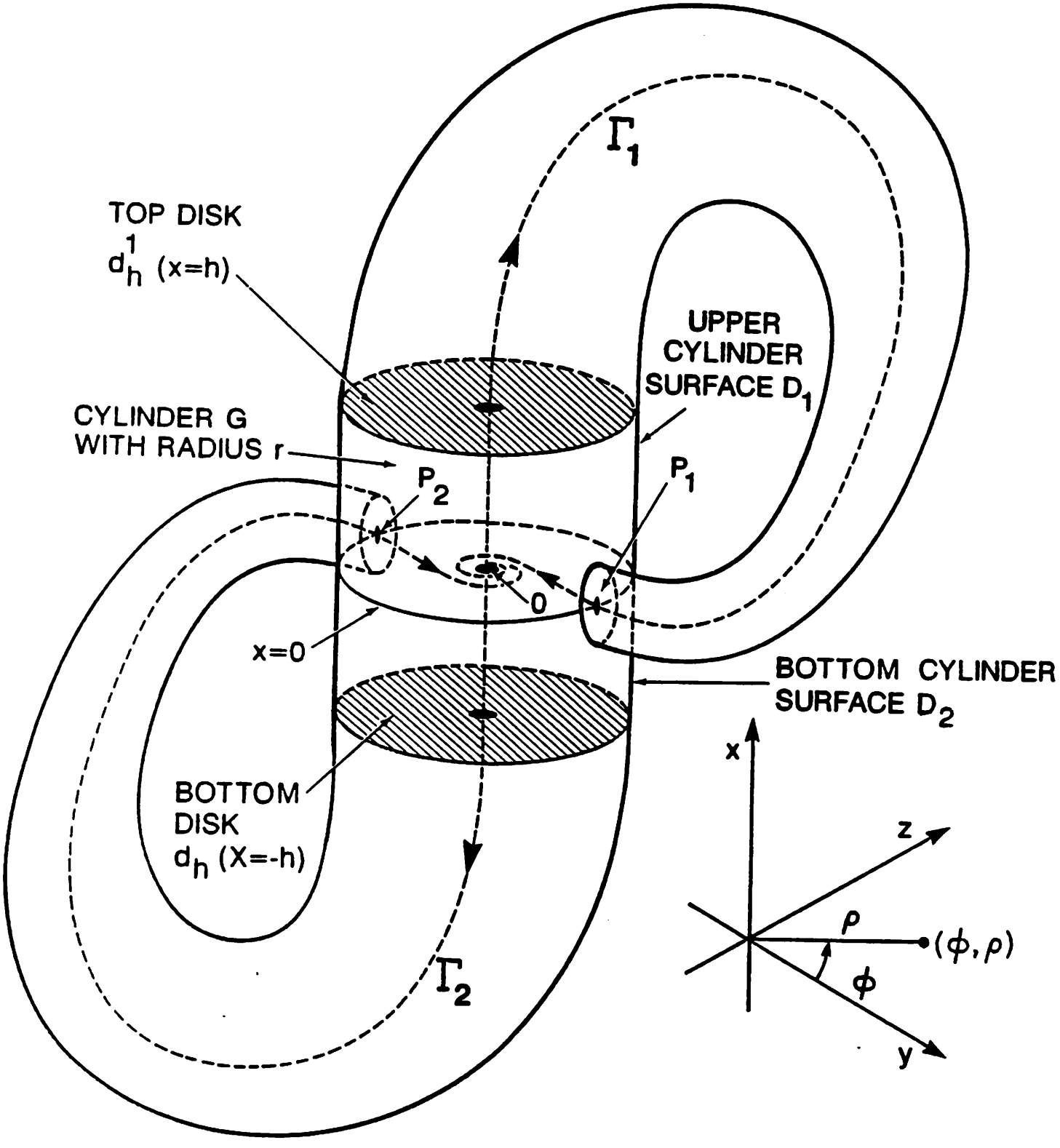
TOP DISK
d_h^1 (x=h)
Γ_1
UPPER CYLINDER SURFACE D_1
CYLINDER G WITH RADIUS r
P_2
P_1
0
x=0
BOTTOM CYLINDER SURFACE D_2
BOTTOM DISK
d_h (X=-h)
Γ_2
x
z
ρ
(ϕ, ρ)
ϕ
y

Fig. 20

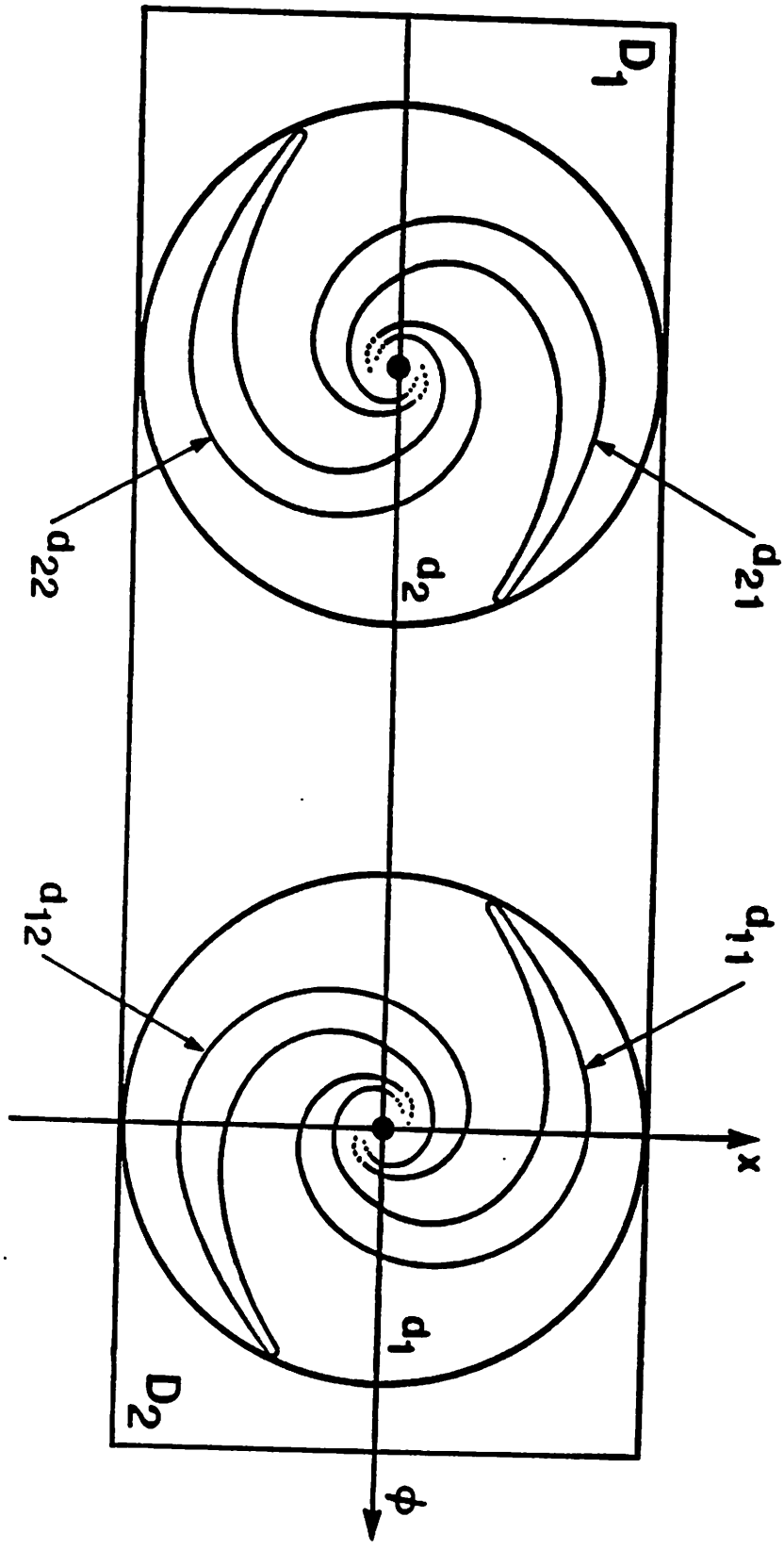

Fig. 2

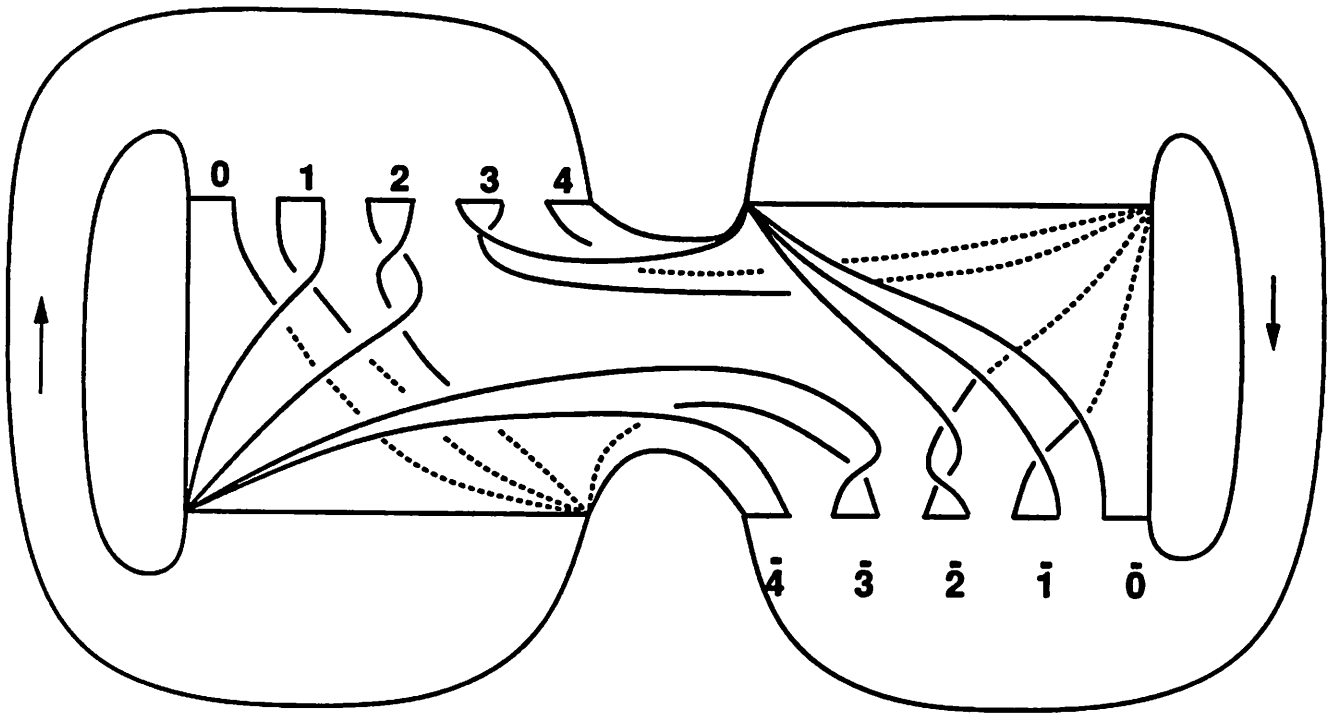

Fig 2:

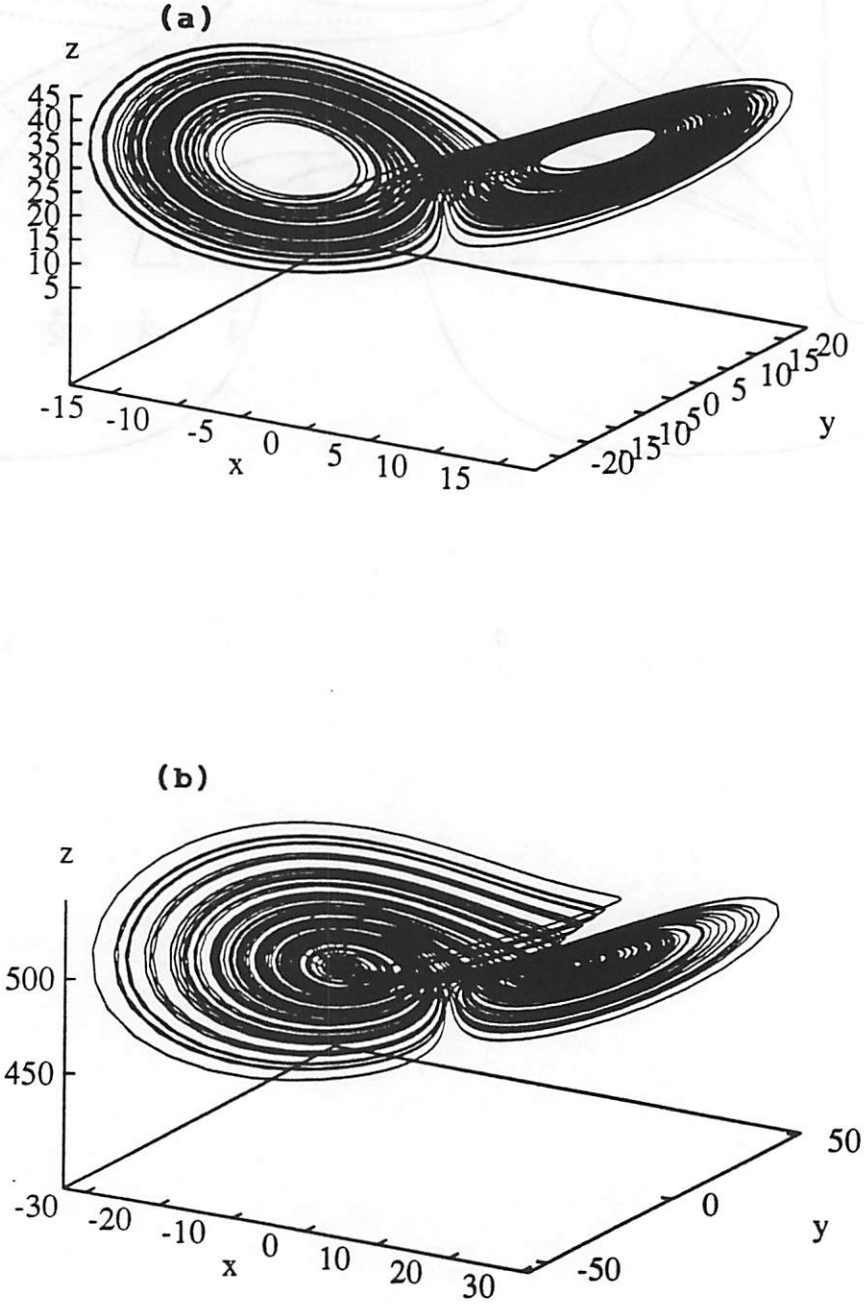
(a)
z
45
40
35
30
25
20
15
10
5
-15
-10
-5
0
5
10
15
x
-20
-15
-10
-5
0
5
10
15
20
y
(b)
z
500
450
-30
-20
-10
0
10
20
30
x
-50
0
50
y

Fig. 23

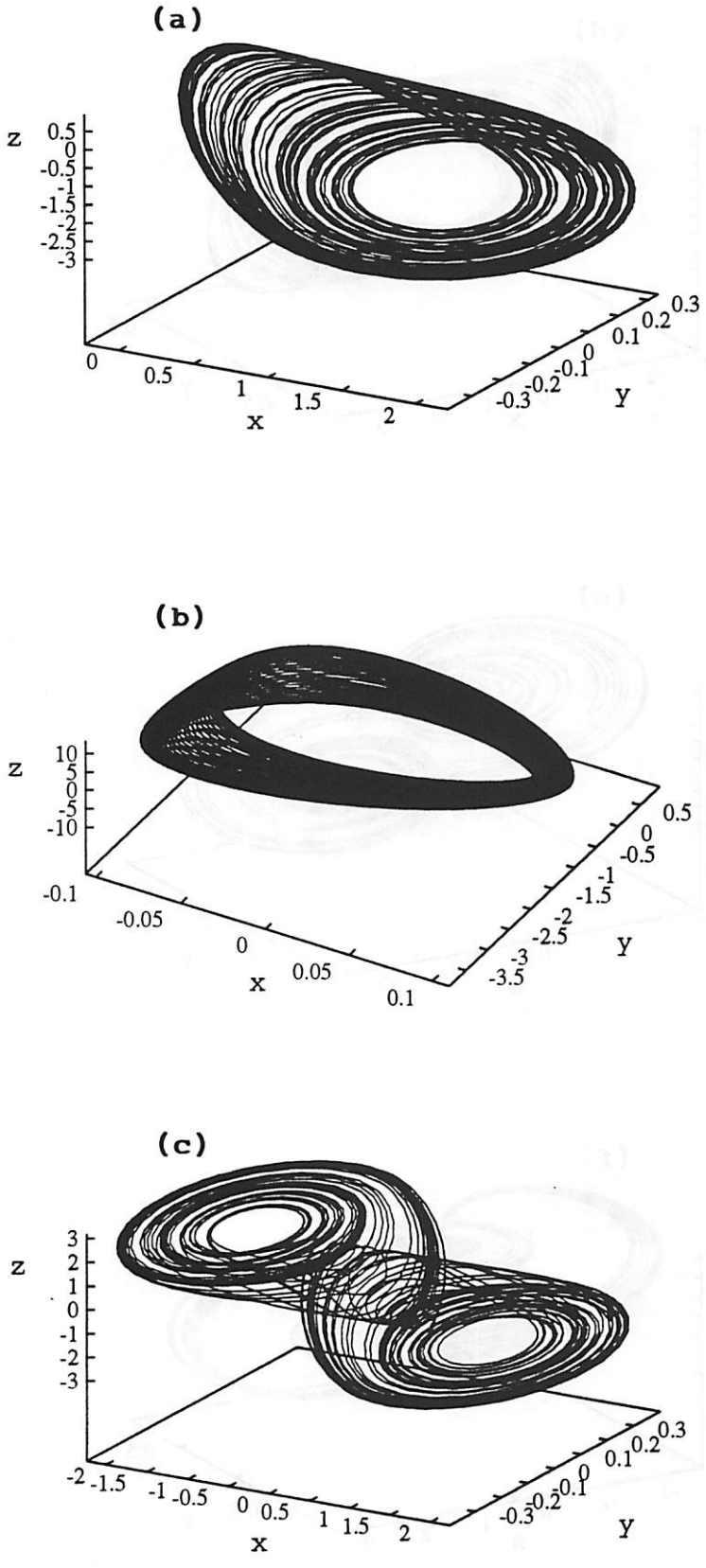
(a)
z
0.5
0
-0.5
-1
-1.5
-2
-2.5
-3
0
0.5
1
1.5
2
x
0.3
0.2
0.1
0
-0.1
-0.2
-0.3
y
(b)
z
10
5
0
-5
-10
-0.1
-0.05
0
0.05
0.1
x
0.5
0
-0.5
-1
-1.5
-2
-2.5
-3
-3.5
y
(c)
z
3
2
1
0
-1
-2
-3
-2
-1.5
-1
-0.5
0
0.5
1
1.5
2
x
0.3
0.2
0.1
0
-0.1
-0.2
-0.3
y

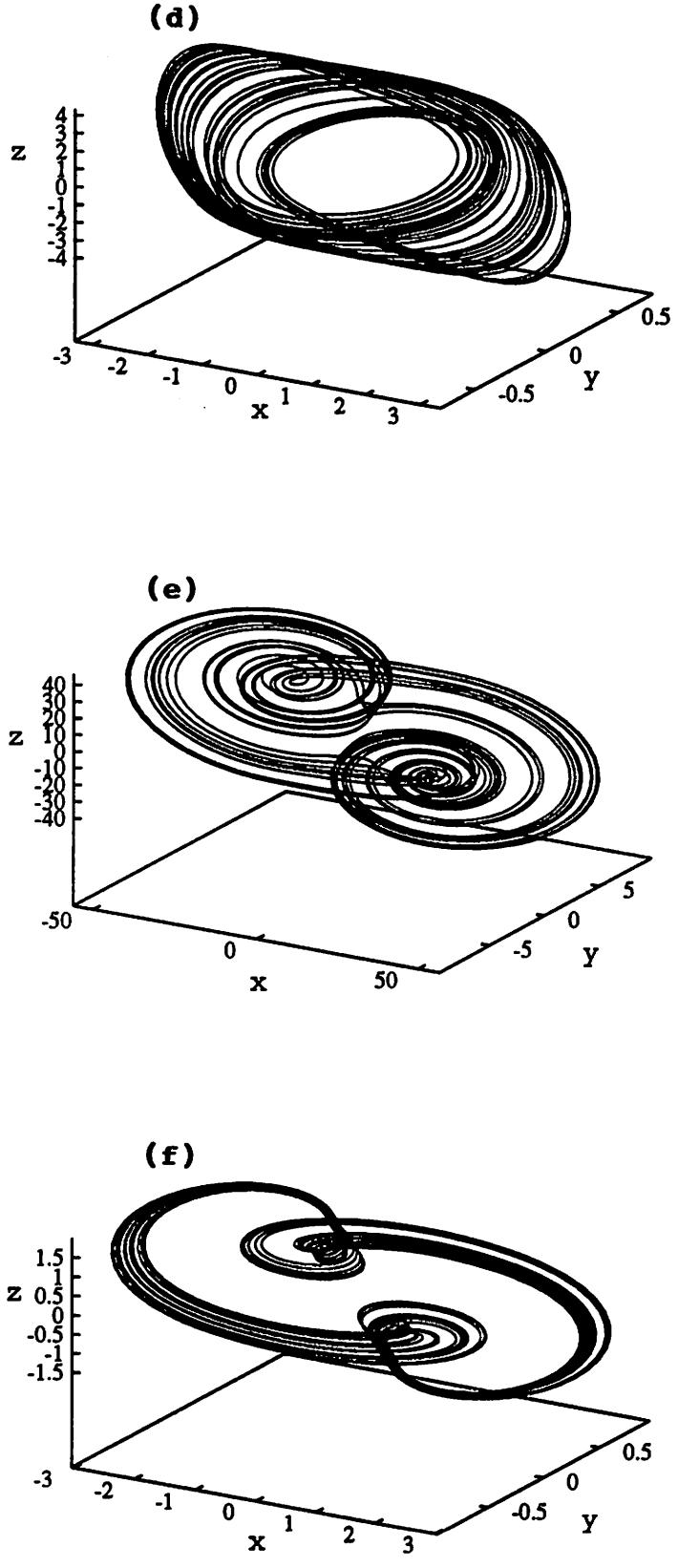
(d)
z
4
3
2
1
0
-1
-2
-3
-4
-3
-2
-1
0
1
2
3
x
0.5
0
-0.5
y
(e)
z
40
30
20
10
0
-10
-20
-30
-40
-50
0
50
x
5
0
-5
y
(f)
z
1.5
1
0.5
0
-0.5
-1
-1.5
-3
-2
-1
0
1
2
3
x
0.5
0
-0.5
y